Collateral sensitivity counteracts the evolution of antifungal drug resistance in *Candida auris.*

Hans Carolus[1,+], Dimitrios Sofras[1], Giorgio Boccarella[2,3], Stef Jacobs[1], Vladislav Biriukov[4,5], Louise Goossens[1], Alicia Chen[1], Ina Vantyghem[1], Tibo Verbeeck[1], Siebe Pierson[1], Celia Lobo Romero[1], Hans Steenackers[8], Katrien Lagrou[9], Pieter van den Berg[2,3], Judith Berman[10], Toni Gabaldón[4-7], Patrick Van Dijck[1,11,+].

[1] Laboratory of Molecular Cell Biology, Department of Biology, KU Leuven, Belgium
[2] Evolutionary Modelling Group, Department of Biology, KU Leuven, Belgium
[3] Evolutionary Modelling Group, Department of Microbial and Molecular Systems, KU Leuven, Belgium
[4] Barcelona Supercomputing Centre (BSC-CNS), Spain
[5] Institute for Research in Biomedicine (IRB Barcelona), The Barcelona Institute of Science and Technology, Spain
[6] Catalan Institution for Research and Advanced Studies (ICREA), Spain
[7] CIBER de Enfermedades Infecciosas, Instituto de Salud Carlos III, Spain
[8] Centre for Microbial and Plant Genetics, Department of Microbial and Molecular Systems, KU Leuven, Belgium
[9] Laboratory of Clinical Microbiology, KU Leuven, Belgium
[10] Shmunis School of Biomedical and Cancer Research, Tel Aviv University, Israel
[11] KU Leuven One Health Institute, KU Leuven, Belgium
[+] Address correspondence to Hans Carolus (hans.carolus@kuleuven.be) and Patrick Van Dijck (patrick.vandijck@kuleuven.be)

Abstract

Antifungal drug resistance represents a significant global health threat necessitating new treatment strategies. Due to the limited classes of antifungal drugs, we investigated collateral sensitivity (CS), where resistance to one drug increases sensitivity to another, and cross-resistance (XR), where one drug resistance reduces susceptibility to multiple drugs. These dynamics can guide treatment redesign to impede resistance development but have not been systematically explored in pathogenic fungi. Here, we used experimental evolution and mathematical modelling of *C. auris* population dynamics during cyclic and combined drug exposures and found that CS-based drug cycling can effectively prevent the emergence of drug resistance. Additionally, we found that a drug that exerts CS can eliminate resistant subpopulations, highlighting the potential for CS-based treatment switches to eliminate established resistance. Furthermore, we show that some CS trends are robust among different strains and resistance mechanisms. Overall, these findings provide a promising direction for improved antifungal treatment approaches.

Introduction

Invasive fungal infections annually affect 6.5 million people worldwide and are attributed to 3.8 million deaths[1]. Despite this, pathogenic fungi suffer neglect in research, the public health sector, and the pharmaceutical industry, resulting in stagnation of the antifungal development pipeline[2-5]. Only four major classes of antifungals are currently available to treat systemic infections: azoles, echinocandins, polyenes and nucleoside analogues[5]. Additionally, antifungal drug resistance rates are on the rise, fuelled by the emergence of novel multidrug-resistant (MDR) species like *Candida auris*[6,7], an opportunistic fungal pathogen first described in 2009[8]. Since then, *C. auris* emerged on all inhabited continents, causing nosocomial outbreaks with high mortality rates[9,10]. Overall, 90% of *C. auris* isolates are resistant to at least one of the four antifungal drug classes, while 30 to 40% are resistant to two drugs or more[9,11,12]. There is an immediate demand for novel therapeutic approaches to combat MDR fungi such as *C. auris*, utilizing clinically approved drugs to ensure their swift availability for clinical application.

Collateral sensitivity (CS), the process in which resistance to one drug confers increased susceptibility to another drug, has been studied in bacterial and cancer cells, where CS-based combination therapy and drug cycling were found to prevent the development of drug resistance and to improve treatment efficiency[13-17]. Since its first identification in 1952[18], several studies have shown the usefulness of CS-based drug cycling in either preventing or reducing drug resistance in bacterial populations[13,19-25]. The mechanism behind CS-based cyclic therapy is that a switch to a CS-exerting drug eradicates resistant subpopulations more than susceptible subpopulations, but cyclic treatment has also been implicated beyond the concept of CS, based on the premise that switching to another treatment relieves the selective pressure for resistance development temporarily and thus slows down resistance evolution[26,27].
Combination treatment can also limit drug resistance development, as shown byseveral studies in bacteria and parasites[14,28-30]. Combination therapy is not commonly used for fungal infections, except for the combination of amphotericin B and flucytosine for treating severe cryptococcosis[31,32]. The combined administration of flucytosine, polyenes, azoles or echinocandins, or combinations of those drugs with repurposed antifungal agents have shown promise against *C. auris*[33,34]. The effect of combination therapy on resistance evolution has not been studied systematically in fungi, although trade-offs have been suggested to minimize resistance evolution in antifungal drug combinations[35].

Neither CS, nor CS-based treatments have been explored in pathogenic fungi. Thus, we systematically investigated CS and cross resistance (XR) dynamics and tested whether CS or XR-inducing drug pairs could respectively decrease or increase the evolution of resistance *in vitro*, using experimental evolution in cyclic and combined drug adminustration, and *in silico* using mathematical modelling of treatment in a virtual patient. Additionally, we asked if switching to treatment with a CS-exerting drug can eradicate a resistant subpopulation of cells in competitive fitness experiments. At last, we evaluated the robustness of CS trends in different strains from different *C. auris* clades with different mechanisms of acquired resistance.

Results

Resistance evolution is drug-dependent but often dose-independent

C. auris Clade I type strain B8441 (AR0387), was exposed to 9 different antifungal drugs to select for resistance: three azoles: posaconazole (POS), fluconazole (FLU) and ketoconazole (KTO); three echinocandins: micafungin (MCF), caspofungin (CAS) and anidulafungin (ANF); the nucleoside analogue flucytosine (5FC); the polyene amphotericin B (AMB) and the allylamine terbinafine (TRB) as shown in **Table 1**. Azoles were selected to include a representative imidazole (ketoconazole), and a first (fluconazole) and second (posaconazole) generation triazole[36]. Micafungin, caspofungin and anidulafungin represent the echinocandins used most frequently to treat candidemia[37].

We evolved the drug susceptible parental strain to obtain adaptors with acquired drug resistance by performing serial transfer (1/10 dilution) of 60 populations into fresh medium with drug every 48h for 14 days (see schematic, **Figure 1A**). For each of the 9 drugs, we used four different drug concentrations, based on the susceptibility of the parental strain: 1xMIC_{50}, 2xMIC_{50}, 4xMIC_{50} and 8xMIC_{50}. After 14 days of drug exposure, relative drug susceptibility was evaluated in 24 single colony adaptors, isolated from 24 independent drug exposed populations (i.e. 6 populations per drug dose). The analysis of independently evolved adaptors increases the probability of isolating diverse resistance-conferring genotypes, enabling more robust conclusions.

Due to distinctive drug-dependent susceptibility profiles (see **Table 1** and **Figure S1**, Supplementary), we express altered drug susceptibility as the resistance ratio RR = susceptibility (evolved adaptor) / susceptibility (parental strain). We use the RR based on both the MIC_{50} and the area under the growth – vs – drug concentration curve (AUC), obtained from broth dilution assays (BDA). The AUC was the preferred metric for susceptibility phenotyping, as it provides a cumulative growth measure that can detect subtle variation in susceptibility profiles, including differential growth in the supra-MIC_{50} and sub-MIC_{50} ranges.

In **Figure 1B** (and **Table S1,** Supplementary), the RR(AUC) of 24 (or less, in the case of population extinction) adaptors per drug after experimental evolution is shown. Although the selective pressure was relative to the parental MIC_{50} and thus equal for all drugs, different drugs caused different trends in evolutionary outcome. Population extinction was observed at higher doses (>MIC_{50}) of flucytosine and amphotericin B. Resistance [RR(AUC)>1] was acquired in 100% of all tested adaptors except those exposed to ketoconazole (72.7% resistant), flucytosine (42.86% resistant) and terbinafine (79.2% resistant). No clear dose-dependent effects were observed, except for flucytosine-exposure which yielded resistant adaptors only at high doses (4xMIC_{50} and 8xMIC_{50}). Comparing the outcome between drugs of the same class revealed a lower level of resistance in adaptors exposed to ketoconazole, compared to posaconazole and fluconazole (**Figure 1B),** although this trend was less pronounced based on MIC_{50} measurements (**Figure S2,** Supplementary). For echinocandins, the level of resistance

development was high for all drugs, albeit significantly lower for caspofungin compared to micafungin and anidulafungin based on RR(AUC) (**Figure 1B**). Based on MIC_{50} however, the median RR of caspofungin adaptors was 32 (**Figure S2** and **Table S1,** Supplementary). This discrepancy between RR(AUC) and RR(MIC_{50}) for caspofungin is due to the fact that the parental strain shows supra-MIC or paradoxical growth (also known as the *eagle effect*[38]) in caspofungin but not in micafungin and anidulafungin. This is a phenomenon commonly observed in *in vitro* susceptibility measurements of caspofungin for *Candida* species, including *C. auris*[39]. The paradoxical growth of the parental strain inflates the baseline AUC for caspofungin yielding lower relative RR(AUC) values compared to micafungin and anidulafungin, in which paradoxical growth is absent (**Figure S1,** Supplementary).

Resistance can lead to collateral sensitivity and cross-resistance

Relative susceptibility to 11 antifungal drugs and 7 repurposed drugs, shown to affect *C. auris* in prior reports[40-42] (**Table 1**), was measured in six independent resistant [RR(AUC) > 1] adaptors per drug to assess collateral sensitivity (CS; RR<1) and cross resistance (XR; RR>1). All six amphotericin B-resistant adaptors were CS to all three echinocandins, flucytosine and geldanamycin (**Figure 1C**). Additionally, flucytosine-resistant and fluconazole-resistant adaptors were CS to micafungin, while some caspofungin-resistant, anidulafungin-resistant, fluconazole-resistant and ketoconazole-resistant adaptors were CS to flucytosine. The remaining CS phenotypes were either mild (0.5<RR<1) or adaptor-specific.
XR and MDR was common amongst drugs of the same class (e.g., the azoles and echinocandins) and between drugs of different classes such as the azoles and echinocandins, and the azoles and amphotericin B (**Figure 1C**).
Interestingly, adaptors resistant to most of the non-conventional or repurposed antifungal agents did not exhibit XR. The only clear example of XR (i.e. RR>2) was in one amphotericin B-resistant adaptor that was XR to diiodohydroxyquinoline (DIH). Additionally, the overall MIC_{50} values of both parental strain and evolved adaptors (including MDR adaptors), was low for most non-conventional drugs (**Figure 2** and **Table S3,** Supplementary). The rather low MIC_{50} and the absence of XR of these agents in resistant and MDR adaptors shows that several repurposed agents are promising therapeutic leads, especially when compared to the extensive inter-class XR observed between the major antifungal drug classes (**Figure 1C**).

Most of the CS and XR trends based on RR(AUC) (**Figure 1C**) agreed with observations based on RR(MIC_{50}) (**Figure S2**, Supplementary). Nevertheless, the parameter for assessing the RR can affect conclusions regarding XR and CS, as some trends seen with RR(AUC) are not detectable for RR(MIC_{50}). In fact, some resistant adaptors are XR based on RR(AUC), yet they exhibit CS to these drugs based on RR(MIC_{50}) and vice versa. Examples are: caspofungin-resistant adaptors that show XR for posaconazole by RR(AUC) but were CS by RR(MIC_{50}); and two amphotericin B-resistant adaptors were XR for all azoles by RR(AUC) but were CS by RR(MIC) (**Figure 1C** vs **Figure S2,** Supplementary). This is due to differences in supra-MIC growth, or drug tolerance. Drug tolerance can be defined as the growth of a subpopulation of cells in drug concentrations higher than the MIC, and is distinct from drug resistance, which is an increase of MIC[43]. Adaptors that show a relative decrease in MIC [RR(MIC_{50}<1] but show

increased growth over all drug concentrations [RR(AUC)>1] can therefore be considered less drug-resistant but more drug-tolerant. Thus, CS and XR can work at the level of both resistance and tolerance, emphasizing the importance of susceptibility parameter choice in the evaluation of CS and XR.

Collateral sensitivity-based drug cycling can prevent resistance

Next, we compared the effects combined drug administration and a 4-day drug cycling regimen (switching between drugs every 4 days), on the emergence of drug resistance in experimental evolution of the naïve parental strain. This was done for CS drug pairs amphotericin B & caspofungin, amphotericin B & flucytosine, amphotericin B & geldanamycin; and the XR drug pair amphotericin B & posaconazole. In the experimental evolution assay, 60 populations were evolved in 4 different drug dose combinations: i.e. combining or cycling two drugs at 1xMIC_{50} or 2xMIC_{50} concentrations each. An exception was made for geldanamycin in which 1 µg/ml and 2 µg/ml were used, as the parental strain did not show a measurable MIC_{50} for geldanamycin within the tested range (**Table 1** and **Figure S1,** Supplementary), and for flucytosine, in which 4xMIC_{50} and 8xMIC_{50} concentrations were used as those were the only dose regimens that yielded resistant adaptors during single drug experimental evolution (**Figure 1B** and **Table S1,** Supplementary). The experimental evolution assay was similar to experimental evolution in single drug exposure, except that cultures were washed between the administration of drug 1 and drug 2 in the cycling protocol (see *Methods*).

After passaging, we isolated 6 single colony adaptors per drug treatment/dose, yielding 24 adaptors (conform experimental evolution in single drug exposure, **Figure 1A**), in which we evaluated relative susceptibility changes to both drugs the adaptors were evolved in, shown in **Figure 3A and 3B.**

Cycling of amphotericin B & geldanamycin significantly reduced the level of resistance to amphotericin B, while amphotericin B & caspofungin cycling reduced resistance to both drugs, compared to exposure to either drug alone. Cycling of amphotericin B & flucytosine did not reduce the level of resistance to amphotericin B but it did significantly reduce resistance to flucytosine, although the level of flucytosine resistance in some adaptors remained high.
Combined administration of amphotericin B & geldanamycin significantly reduced the emergence of amphotericin B resistance and amphotericin B & caspofungin reduced the emergence of caspofungin resistance but not amphotericin B resistance. Interestingly, resistance to caspofungin was only acquired in conditions where low amphotericin B and high caspofungin concentrations were combined. Drug dosage and pharmacokinetic properties of drugs might be important variables in CS-based treatment, presenting an interesting area for future research.

Drug cycling of the reciprocal XR drug pair posaconazole and amphotericin B did not significantly affect resistance development but combined administration led to a significant decrease in amphotericin B resistance development compared to single amphotericin B exposure and cyclic exposure (**Figure 3B**). This might be the result of drug interactions.

Overall, the evaluation of RR(AUC) (**Figure 3A-B**) and RR(MIC_{50}) (**Figure S3,** Supplementary) identified similar trends, except for a significant reduction of amphotericin B resistance in the combined administration of amphotericin B and caspofungin based on RR(MIC_{50}), which was not detected based on RR(AUC). Notably, RR(MIC_{50}) showed a significant reduction in posaconazole resistance in both cyclic and combined administration of amphotericin B and posaconazole, yet posaconazole-resistant adaptors were detected in all conditions.

Next, we further investigated the implications of cyclic therapy with the most promising CS drug pair: amphotericin B and caspofungin. We used a mathematical model based on an ordinary differential equation (ODE) framework, to predict the *in vivo* emergence of resistance in amphotericin B & caspofungin drug cycling regimens relative to treatment with only one of the two drugs (**Figure 3D**). The model includes *in vivo* pharmacokinetic and immune killing effects and was based on an *in vitro* model that aligned with empirical outcomes of the *in vitro* experimental evolution assays (**Table S5** and **Figure S4**, Supplementary). Besides drug susceptibility and CS of the parental strain and resistant adaptors, parameters such as growth rate and basal mutation rate were evaluated and incorporated in the model. The growth rate was estimated from growth curves using the Easy Linear Method[44], while the basal mutation rate was determined with a fluctuation assay. See *Methods* for a detailed description of the model, parameter estimations and included values.

Figure 3C depicts how this model predicts that the shorter the amphotericin B and caspofungin cyclic drug exposure is, the smaller the viable population sizes are, with a total absence of resistant (or susceptible) cell populations in all simulations during daily (24h) cycling. Model simulations predicted that drug-susceptible cell populations are eradicated at a slower rate during cyclic therapy compared to amphotericin B monotherapy, yet the CS of amphotericin B-resistant cells to caspofungin effectively eradicates the emergence of amphotericin B-resistant subpopulations within 8 days of treatment (**Figure 3D**).

Collateral sensitivity can select against resistant subpopulations

Our results indicate that CS-based cycling can *prevent* the evolution of resistance. Next, we asked if CS-based drug administration can *decrease* or *clear* resistance once it has already been established. We evaluated whether the administration of a CS drug to a mixed population of susceptible and resistant cells can eliminate the resistant sub-population in competitive fitness experiments in which we tracked the size of the susceptible and resistant sub-populations over time. The drug-susceptible parental strain was tagged with a nourseothricin (NTC) resistance marker (*NAT*, which encodes a nourseothricin N-acetyl transferase), enabling selected growth on NTC containing medium. This approach first required the identification and validation of a neutral locus for the stable genomic integration of the NAT marker.

We identified an intergenic region (further referred to as ‘CauNEUT’) of 538bp in *C. auris* strain B8441, based on a syntenic intergenic region of 550bp between orf19.1961

(C5_01090C_A) and *GDS1* (C5_01080C_A) in *C. albicans*, termed CaNEUT5L[45] (**Figure S5,** Supplementary). TNAT knock-in transformants (wt^{NAT_A} and wt^{NAT_B}) did not show fitness trade-offs in broth dilution assays (**Figure S6,** Supplementary) and growth curves in different conditions (**Figure S7,** Supplementary). We propose that CauNEUT might be valuable for other applications such as CRISPR or fluorescent tagging, to avoid integrating the genetic cassette into potentially important loci[46-49].

Next, we used a tagged wt^{NAT} strain (wt^{NAT_A} in **Figure S6-7,** Supplementary) as the drug-susceptible strain in competitive fitness experiments: wt^{NAT} was mixed 50:50 with each of the six independently evolved amphotericin B-resistant adaptors and grown in drug-free, amphotericin B, caspofungin or flucytosine conditions (drugs at 1xMIC_{50} of the wt strain) for eight days.

In caspofungin, and to a lesser extent in flucytosine, wt^{NAT} cells often outcompeted the amphotericin B-resistant subpopulations, while in amphotericin B, the amphotericin B-resistant adaptors dominated (**Figure 4**). In the drug-free condition, wt^{NAT} cells outcompeted some amphotericin B-resistant populations (**Figure 4A**), which may reflect the fitness trade-offs of amphotericin B resistance reported for *Candida* sp.[50-53]. Overall, caspofungin administration was most effective in reducing the amphotericin B-resistant subpopulation: on average, amphotericin B-resistant cells made up less than 6% of the total population after 8 days with extinction of this population in most cases (**Figure 4C).** Thus, using a CS approach can eliminate drug-resistant subpopulations of cells.

Collateral sensitivity can be genotype and background-independent

Both the mechanism of drug resistance and strain genetic background can influence CS and XR phenotypes[54]. To investigate the robustness of CS and XR, we 1) analysed the mechanisms of resistance in the six amphotericin B-resistant adaptors of the Clade I parental strain as used in the experiments above, and 2) mapped CS/XR to 7 dugs in 13 additional amphotericin B-resistant adaptors from *C. auris* Clade II, III and IV from this and other studies[50,52] (**Figure 5**). The adaptors were selected to represent each of the four major mechanisms of acquired resistance to amphotericin B known for *C. auris*[50,52,55,56] in the four major clades of *C. auris*[57]. *ERG6* mutants have been identified to confer acquired amphotericin B resistance in clinical settings[56].

Based on RR(AUC), all amphotericin B-resistant adaptors, regardless of clade or mechanism of resistance, were CS to caspofungin and geldanamycin (**Figure 5**). Moreover, CS was strong for all three echinocandins and for all the mechanisms of amphotericin B resistance except for some Clade IV adaptors, which were not CS to micafungin (adaptors 16 and 18) or anidulafungin (adaptors 13, 15 and 16). For flucytosine, the response was clade-specific: all Clade I adaptors were CS, while Clade II and most Clade III and Clade IV adaptors were XR to flucytosine. XR for azoles in amphotericin B-resistant adaptors was background or genotype

specific, but the majority of adaptors were XR to posaconazole. Adaptors with variation in mevalonate pathway effectors (adaptors 16-18) were CS rather than XR to both posaconazole and fluconazole.

The CS/XR landscape based on RR(AUC) and RR(MIC_{50}) was significantly different for some drugs (**Figure 5** vs **Figure S8,** Supplementary). Strikingly, more echinocandin XR than CS was observed for Clade III and Clade IV adaptors, based on RR(MIC_{50}). As noted above, relative changes in drug tolerance rather than resistance could underly these differences between RR(MIC_{50}) and RR(AUC). Due to these biased results, we further investigated changes in drug tolerance and resistance by performing ETEST® (bioMérieux) susceptibility assays for echinocandins in all amphotericin B-resistant adaptors **(Figure S10,** Supplementary). The evaluation of RR(MIC) based on ETEST identified CS towards most echinocandins in most adaptors, with some exceptions. Specifically, Clade IV adaptors deviated from the main CS trend, exhibiting caspofungin XR rather than CS based on ETEST MIC values. This is probably due to the high drug tolerance (identifiable by growth within the growth inhibition ellipse of the ETEST) of the parental strain for this drug (**Figure S10C,** Supplementary). The comparison of RR(MIC) heatmaps of broth dilution assays (BDA) (**Figure S8,** Supplementary) and ETEST **(Figure S10D,** Supplementary) highlights important assay-dependent differences, which stresses the importance of the method used for evaluating CS and XR.

In addition to determining changes in MIC, we qualitatively evaluated echinocandin tolerance in all amphotericin B-resistant adaptors using the ETEST assay by visually comparing the growth within the inhibition ellipse after 72h of incubation in adaptors and their parental strains (**Figure S10F,** Supplementary). We note that CS can be evident at both the resistance and tolerance level (e.g. most Clade III adaptors) or it can appear as a decrease in MIC but not tolerance (e.g. Clade II adaptor and most Clade IV adaptors for anidulafungin) or vice versa (e.g. Clade IV adaptors 13-15 for caspofungin). Tolerance-based CS to caspofungin was present in most adaptors, but we also observed a gain of anidulafungin and/or micafungin tolerance in some Clade IV adaptors. Interestingly, there is no clear correlation between the different parameters of resistance and tolerance [i.e. BDA based RR(AUC) (**Figure 5**) and RR(MIC_{50})(**Figure S8,** Supplementary); ETEST based RR(MIC) (**Figure S10D,** Supplementary) and differential tolerance (**Figure S10E**, Supplementary)]. This reveals an unexpected complexity of CS and XR phenotypes and stresses the importance of the susceptibility parameters and assays used for evaluating these phenotypes.

In conclusion, although the extent of CS can depend on the drug-, mutant-, strain (clade) background - or susceptibility-testing method used, several general and robust trends were clear: collateral sensitivity is seen for amphotericin B-resistant genotypes and clades for both caspofungin and geldanamycin. In addition, the majority of amphotericin B-resistant adaptors showed CS to all three echinocandins.

Discussion

Collateral sensitivity is a promising, yet understudied phenomenon in pathogenic fungi. Here, we used *in vitro* experimental evolution to acquire resistant adaptors and identify collateral sensitivity towards several antifungal agents. We identified robust trends of CS and show that CS can be leveraged to both prevent the emergence and reduce the presence of antifungal drug resistance.

When exposed to a single drug, resistance was usually acquired within 14 days of exposure to drug concentrations as low as the MIC_{50}. The ease of echinocandin resistance development is concerning, given that echinocandins are currently the first-line treatment for systemic *C. auris* infections[58]. In amphotericin B, extinction was common at drug concentrations higher than the parental strain MIC_{50}, with only rare surviving populations harbouring resistant adaptors. This is most likely due to the strong fungicidal effect of amphotericin B and fitness costs associated with amphotericin B resistance[50]. Flucytosine resistance only evolved in higher concentrations, which suggests that acquired resistance carries a fitness cost. Such fitness trade-offs have been identified in *S. cerevisiae* and *C. neoformans* before[59].

Several repurposed antifungal agents were effective against both drug-susceptible, drug-resistant and MDR *C. auris* adaptors. Nitroxoline, alexidine dihydrochloride, ciclopirox ethanolamine and diiodohydroxyquinoline had overall low MIC_{50} values for the parental strain (compared to conventional antifungals) and most resistant adaptors while exhibiting fungicidal activity within the tested range. The mechanisms of action, such as iron chelation for nitroxoline, ciclopirox ethanolamine and diiodohydroxyquinoline[60-62], are distinct from those of the conventional antifungals, consistent with their effectiveness on resistant and MDR adaptors. While most of these agents are not readily available for treating systemic infections due to pharmacological constraints, their distinct mode of action, fungicidal nature and efficacy against MDR adaptors, warrants further investigation into their potential for treating MDR fungal pathogens.

Although XR to drugs from the same antifungal class is common in *Candida* sp.[63-67], exceptions have been reported, like *FKS* mutations that confer resistance to one or two but not all echinocandins in *C. glabrata*[68], and resistance to fluconazole but not to other azoles like posaconazole in *C. auris*[69,70]. Although intra-class XR was common, we also observed exceptions, suggesting that different resistance mechanisms are at play. In addition, XR between azoles and echinocandins, and between azoles and amphotericin B was common. XR between amphotericin B and azoles is a commonly reported form of MDR in *C. auris*[52], *C. albicans*[71,72], *C. glabrata*[73] and *C. tropicalis*[51,74], in which mutations in genes involved in ergosterol biosynthesis are implicated[52,71-73]. The fact that XR to azoles in amphotericin B-resistant adaptors was dependent on the strain background and the mechanism of resistance, indicates that XR is not simply a function of the mechanism of action of either of the two drugs, and that differences between strains may be very important.

The nature of the test (BDA vs ETEST), susceptibility parameter [RR(AUC) vs RR(MIC)] and phenotype (tolerance vs resistance) are important factors in the evaluation of CS and XR. Our preferred parameter for CS screening is RR(AUC) based on BDA, as it considers differences in both MIC_{50} and supra-MIC_{50} growth, including drug tolerance. Antifungal drug tolerance is distinct from resistance, and does not involve an increase in MIC, but rather a increased capability to grow slowly at higher drug levels. This drug tolerance is thought to contribute to persistent infections[75] and antifungal treatment failure[76,77], but remains understudied compared to drug resistance. The loss or gain of drug tolerance in CS or XR can be an important aspect of treatment success in CS-based therapy.

Irrespective of the susceptibility parameter and testing methods, CS to caspofungin was clearly detected in amphotericin B-resistant adaptors from all four clades of *C. auris.* Similarly, Rybak *et al.* found CS to caspofungin in consecutive clinical isolates of *C. auris* that acquired amphotericin-B resistance via *ERG6* modulation[56]. Later, the disrupted *ERG6* gene was restored by a second mutation, suggesting that the *ERG6* mutation confers a significant fitness trade-off and is thus selected against. In this study we confirm that amphotericin B-resistant *ERG6* mutants commonly show CS to caspofungin and are actively selected against in a competitive fitness experiment during caspofungin treatment. In a recent study *ERG6* modulation came forward as the most common mechanism of acquired amphotericin B resistance in *C. auris,* and it was linked to specific fitness trade-offs[50]. Additionally, a mutation in *CDC25* was identified that compensated for fitness trade-offs linked to *ERG6* disruption[50]. Similarly, variation in *CDC25* in the *ERG6* mutants reported by Rybak *et al.*[56] might have facilitated the selection for resistant mutants[50]. Compensatory evoluton presents an unexplored aspect of antifungal drug resistance and might play an important role in CS-based therapy.

Fitness trade-offs of resistance have been demonstrated to cause CS in bacteria[78-80]. CS mediated by such trade-offs could potentially be explained in part by looking at the mode of action of the drugs involved. For example, the molecular chaperone Hsp90 regulates stress homeostasis by stabilizing a myriad of stress-regulating effectors, including calcineurin and protein kinase C, two signal transducers that mitigate cell wall stress and membrane stress exerted by drugs like echinocandins and polyenes respectively[81]. Amphotericin B-resistant cells are more susceptible to several stressors[50] and more dependent on Hsp90 compared to susceptible cells[51], thus making them more vulnerable for the stress induced by the Hsp90 inhibitor geldanamycin, and potentially echinocandins. Previous studies have demonstrated the increased sensitivity of amphotericin B-resistant cells to geldanamycin, and thus CS, in *C. albicans* and *C. tropicalis*[51]. The Hog1 MAP-kinase is another client protein of Hsp90 that negatively regulates the expression of ergosterol biosynthesis genes and membrane ergosterol levels in *S. cerevisiae* and *C. neoformans*[82,83]. In a recent study, perturbations of the *C. auris* Hog1-signaling pathway in *C. auris* conferred resistance to caspofungin and to cell wall stress inducing agents such as CFW and CR, while SDS mediated membrane stress sensitivity was increased[84]. If this effect is reciprocal, and amphotericin B resistance is dependent on Hog1 signal transduction but echinocandins downregulate it, this presents another putative mechanism of echinocandin CS in amphotericin B-resistant strains. This is supported by the observation that *HOG1* deletion strains are hypersensitive to amphotericin B in *C. albicans*[51].

Beyond stress homeostasis, additional mechanisms can underly the CS. For example, as ergosterol is crucial for maintaining cell membrane integrity, reduced ergosterol levels or alternative sterols due to *ERG*-gene modulation potentially compromise the stability of lipid rafts and function of membrane-associated proteins such as Fks1, rendering amphotericin B-resistant cells more susceptible to echinocandins. The combination of mutations in *FKS* and *ERG3* has been observed in *C. auris*[52], *C. glabrata*[85], *C. parapsilosis*[86], *C. lusitaniae*[87] and *C. albicans*[88], which suggests that sterol biosynthesis modulation might play a role in echinocandin activity and resistance. This could perhaps explain why amphotericin B-resistant adaptors with modified membrane sterols are more sensitive (CS) to echinocandins.
In bacteria, various other mechanisms have been hypothesized to play a role in CS, including increased drug uptake, reduced efflux, enhanced chemical activity of drugs, alterations in regulatory pathways or enhanced binding to antibiotic targets[89]. Which of these and other proposed mechanisms, or a combination hereof, contribute to the CS phenotypes we observe in this study remains to be elucidated.

Experimental evolution and modelling results show that cyclic administration of two of the most commonly used antifungal drugs – amphotericin B and caspofungin – can effectively prevent resistance development, while competitive fitness experiments shows that, beyond the "prophylactic" use of CS drug cycling of amphotericin B and caspofungin, the CS-based treatment switch to caspofungin can clear established amphotericin B-resistant sub-populations *in vitro*. In addition, the combined and cyclic administration of amphotericin B and geldanamycin lead to reduced amphotericin B resistance in the experimental evolution assays. Prior research suggested that targeting Hsp90 might impede antifungal resistance development[46,51,81,90-92]. The inhibition of Hsp90 by geldanamycin can reduce azole tolerance[75] and preclude the appearance of azole-resistant cells[91]. A clinical study also found enhanced treatment efficacy and reduced mortality of invasive candidiasis when patients were treated with amphotericin B and a recombinant antibody against *C. albicans* Hsp90[92]. These results underscore the potential use of Hsp90 inhibition together with amphotericin B to prevent the development of drug resistance.

Although the combined administration of amphotericin B and caspofungin significantly reduced the acquisition of caspofungin resistance, several adaptors showed high caspofungin MIC_{50} values. Interestingly, resistance was only detected in adaptors from the low amphotericin B – high caspofungin dose condition, highlighting dose-dependency in CS-based treatment. By contrast, in drug cycling regimens, the emergence of high drug resistance was less frequently motivating the use of CS-based drug cycling rather than combination therapy. It is also important to note that although the level of resistance was significantly lower in most cyclic or combined drug conditions, decreased susceptibility could still be detected. Whether these levels of resistance can challenge antifungal treatment in an *in vivo* and clinical context, remains to be investigaterd.
Despite the fact that XR was detected between amphotericin B and posaconazole exposed adaptors, the combined administration of both drugs yielded a significant reduction rather than increase of amphotericin B resistance, compared to single drug administration. These results

highlight the importance of, and need for further empirical research into XR, drug interactions and the effect of combining drugs on resistance development.

In conclusion, CS-based antifungal strategies with clinically available antifungal drugs such as caspofungin and amphotericin B, can prevent and reduce the acquisition of resistance in *C. auris*. In addition to CS-based combination or cyclic treatments, CS and XR trends might guide therapeutic decisions when resistance emerges in monotherapy, although the effect of CS-based treatment switches on established resistant populations remains to be investigated in an *in vivo* and clinical context. While CS and XR dynamics can vary between genotypes and strains, CS can motivate specific treatment switches on individual patient basis, if the CS and XR profile of the infecting strain is known. This may be especially relevant for outbreaks of *C. auris* infections, which are often clonal within a single clinical facility. Such a personalized medicine approach would require continuous monitoring with a highly sensitive, rapid diagnostic test for drug susceptibility.

Methods

Strains and growth conditions

The parental (wild type) strain used in this study was a single colony isolate from clinical strain B8441 (also referred to as AR0387) originating from Pakistan. Strain B8441 can be considered the type strain for *C. auris*, as it is the only curated *C. auris* genome on Candida Genome Database[93] (CGD; candidagenome.org) and one of the most commonly used reference strains in research[9,46,56,57,94-99]. For robustness testing we used wild type and experimentally evolved adaptors from Clade III and IV from Carolus *et al.* (2023)[50] and Clade II from Carolus *et al* (2021)[52]. Susceptibility profiles of all parental progenitors are shown in **Table 1, Figure S1** and/or **Figure S9** (Supplementary). Clade affiliation was confirmed according to Carolus *et al.*[100].

Unless specified otherwise, *C. auris* cells were grown in 5 ml MOPS (4-morpholinepropanesulfonic acid) buffered (pH 7) RPMI 1640 (Thermo Fisher Scientific) medium with 2% glucose, in a shaking (240 rpm) incubator at 37°C. Strains were stocked at -80°C in 20% glycerol and plated on solid YPD (1% yeast extract, 2% peptone, 2% dextrose) agar with 2% glucose at 37°C. For plasmid propagation and cloning the E. coli TOP10F' strain was used. Transformed bacteria were grown in LB (Sigma) medium supplemented with 100 µg/mL ampicillin (Duchefa Biochemie) at 37 °C.

In vitro experimental evolution

Per drug, 60 wells of a round-bottom 96-well polystyrene microtiter plate (Greiner) were inoculated with 10^6 cells in 200 µL RPMI-MOPS medium (pH 7, 2% glucose, 1% DMSO) and drug in 4 different drug concentrations, creating 4 groups of 15 wells per drug concentration. The 4 corner wells were inoculated with the same inoculum but without drug (growth control). The remaining wells of the plate were filled with sterile water. Antifungal drugs in single drug evolution were applied at concentrations of 1xMIC_{50}, 2xMIC_{50}, 4xMIC_{50} and 8xMIC_{50} of the parental wt strain (see **Table 1**). In combination and cyclic drug administration, combinations of 1xMIC_{50} and 2xMIC_{50} drug concentrations were applied, except for flucytosine, for which 4xMIC_{50} and 8xMIC_{50} concentrations were used as resistance development was only detected in these conditions (**Figure 1B** and **Figure S2A** and **Table S1,** Supplementary), and geldanamycin in which 1µg/ml and 2 µg/ml were used as the parental strain did not show a measurable MIC_{50} for geldanamycin within the tested concentration range (**Table 1** and **Figure S1,** Supplementary). In figures and tables, the lowest and highest dose administered is annotated by 'L' and 'H' respectively. The order of dose annotation is the same as the order in which drugs are mentioned in treatment conditions (e.g. AMB-GEL LH: low AMB and high GEL). The experimental evolution assay consisted of 1/10 dilution (20 µL transfer to 180 µL fresh medium at 37°C) of each population every 48 hours. Each experiment consisted of 6 serial transfers and 14 or 16 days (i.e. for drug cycling with a total of 2 times 4-day exposure to each drug). Upon drug cycling therapy, cultures were pelleted by centrifugation of the microtiter plate for 5 min at 5 251xg, washed in sterile PBS, subsequent centrifugation and resuspension in RPMI-MOPS with the new drug. All plates were stored at -80°C after addition of glycerol to a final concentration of 27% per well.

Drug susceptibility testing

Drug susceptibility was assessed by broth dilution assay (BDA) based on CLSI guidelines[101]. Briefly, a 16 µg/ml to 0.0625 µg/ml 2-fold dilution range of drug was prepared in a final volume of 200 µL RPMI-MOPS (pH 7, 2% glucose, 1% DMSO) medium with 100-500 cells (based on OD_{600nm} and serial dilution), seeded in a round-bottom 96-well polystyrene microtiter plate (Greiner). Plates were incubated at 37°C for 48 hours, and growth was assessed spectrophotometrically (OD_{600}) using a Synergy™ H1 microplate reader (BioTek).

Due to distinctive drug-dependent susceptibility profiles, alterations in drug susceptibility are expressed as a ratio relative to the parental wt strain: termed the *resistance ratio (RR)* of the minimum inhibitory concentration of 50% growth (MIC_{50}) and the area under the growth – vs – drug concentration curve (AUC^{BDA}), obtained from BDA. AUC^{BDA} was calculated in GraphPad Prism (v. 10.0.3 (217)) using the trapezoid rule ΔX*([(Y1+Y2)/2]-Baseline], and MIC_{50} was calculated in Microsoft Excel, both based on relative (to drug free) growth profiles averaged over minimum 2 measurements (technical repeats). AUC^{BDA} was the preferred metric for susceptibility phenotyping, as it provides a cumulative growth measure that can detect subtle variation in susceptibility profiles, including differential growth in the supra-MIC_{50} and sub-MIC_{50} ranges (see **Figure S1,** Supplementary).

To estimate the minimum fungicidal concentration (MFC), or the concentration of drug at which 99% of the population does not survive, 2 µL per well was spotted onto YPD agar using a plate replicator and the drug concentration at which no CFUs were detected was assigned the MFC.

Susceptibility to caspofungin, anidulafungin and micafungin was assessed for amphotericin B-resistant adaptors of all three clade isolates by ETEST® (bioMérieux). In short, MOPS buffered (pH 7) RPMI-1640 agar plates (2% glucose) were swapped with a cotton swap dipped in a cell suspension adjusted spectrophotometrically to OD 0.1 (McFarland 0.5). The plates were incubated at 37°C and scans were taken at 48 and 72 h. The MIC value was read at 48 h as the lowest concentration at which the border of the elliptical inhibition zone intercepted the strip, while any growth, such as microcolonies or heteroresistant populations, throughout a discernable inhibition ellipse, was ignored, as per the manufacturer instructions. Relative increased or decreased drug tolerance was identified as an increase or decrease of growth within the growth inhibition ellipse of the ETEST.

Growth analysis

Cultures were diluted in 200 µL RPMI-MOPS (2% glucose) to a final cell concentration of 10^6 cells per well in a flat-bottom 96-well microtiter plate (Greiner). Growth was monitored spectrophotometrically for 48h at 37°C in a Multiskan GO automated plate reader (Thermo Scientific) with intermittent (10 min. interval) pulsed (1 min medium strength) shaking and 30-minute interval measurements. Growth curves were generated based on three replicate measurements (individual wells) of optical density at 600 nm (OD_{600}). Growth rate analysis was performed with the Easy Linear method using the growthrates package (v.0.8.4) in RStudio (v. 2023.06.1+524)[44].

Mutation rate analysis

The basal mutation rate was estimated by rate of Ura3 LoF in a fluctuation assay. *URA3* encodes an orotidine 5'P decarboxylase (ODCase), which converts 5-fluoroorotic acid (5-FOA) into toxic compounds leading to cell death, which enables differential plating of *URA3* LoF mutants on 5-FOA containing medium[102]. The fluctuation assay protocol was based on Burrack *et al.*[99]. In short, 8 single colonies per strain were inoculated individually in a 96 deep-well plate containing 1 mL of RMPI-MOPS (2% glucose) medium. Cultures were serially diluted and plated on YPD and YNB + 5-FOA (1.7 g/L YNB w/o amino acids & w/o ammonium sulphate + 0.1 g/L uridine, 0.1g/L uracil, 5g/L ammonium sulphate, 20 g/L glucose and 1 g/L 5-FOA) agar for CFU enumeration before and after 24h incubation at 37°C. Mutation rate was calculated using the Lea-Coulson median estimator method[103].

Mathematical model

To evaluate the response of *C. auris* populations to CS-inducing antifungal agents amphotericin B (AMB) and caspofungin (CAS), we constructed a mathematical model based on Aulin *et al.*[20], integrating both stochastic and deterministic elements. We used an ordinary differential equation (ODE) framework to model the change in population size of the following subpopulations:

$$\frac{dS}{dt} = S\left(1 - \frac{S + R_{\text{amb}} + R_{\text{cas}}}{10^{B_{\max}}}\right) g_{\max} \times \text{Drug Effect} - j_n S E$$

$$\frac{dR_{\text{amb}}}{dt} = R_{\text{amb}}\left(1 - \frac{S + R_{\text{amb}} + R_{\text{cas}}}{10^{B_{\max}}}\right) (g_{\max} \cdot \text{fit}) \times \text{Drug Effect} - j_n R_{\text{amb}} E$$

$$\frac{dR_{\text{cas}}}{dt} = R_{\text{cas}}\left(1 - \frac{S + R_{\text{amb}} + R_{\text{cas}}}{10^{B_{\max}}}\right) g_{\max} \times \text{Drug Effect} - j_n R_{\text{cas}} E$$

$$\frac{dE}{dt} = q\,(e_{\max} - E) - lE$$

Where: The terms ***S, R_{amb}*** and ***R_{cas}*** denote the susceptible (parental), amphotericin B-resistant and caspofungin-resistant subpopulations respectively. ***B_{max}*** denotes the maximum carrying capacity for populations in the system. ***$g(_{max})$*** is employed to define the maximum growth rate of parental susceptible cells. ***fit*** signifies the relative fitness cost of the resistant strain compared to the parental strain (with range 0-1). The term ***E*** represent the activated immune effector cell population with ***e_{max}*** representing the maximum effectors population size. We considered the activation and decay of immune cells, where ***q*** designates the rate of activation of immune effector cells, whereas ***l*** marks the decay rate of these cells. Lastly, the rate at which cells are killed by immune effector cells is denoted by ***j_n***.

The **Drug effect** for each subpopulation is modelled as follows:

$$D_{\text{eff}}(S) = 1 - \frac{\left(g - \frac{g_{\min_{\text{amb}}}}{g}\right)\left(\frac{C_{\text{amb}}}{MIC_S}\right)^{H_{\text{amb}}}}{\left(\frac{C_{\text{amb}}}{MIC_S}\right)^{H_{\text{amb}}} - g_{\min,\text{amb}}/g} - \frac{\left(g - \frac{g_{\min,\text{cas}}}{g}\right)\left(\frac{C_{\text{cas}}}{MIC_S}\right)^{H_{\text{cas}}}}{\left(\frac{C_{\text{cas}}}{MIC_S}\right)^{H_{\text{cas}}} - g_{\min,\text{cas}}/g},$$

$$D_{\text{eff}}\left(R_{\text{amb}}\right) = 1 - \frac{\left(g - \frac{g_{\min,\text{amb}}}{g\cdot\text{fit}}\right)\left(\frac{C_{\text{amb}}}{MIC_{\text{amb}}}\right)^{H_{\text{amb}}}}{\left(\frac{C_{\text{amb}}}{MIC_{\text{amb}}}\right)^{H_{\text{amb}}} - g_{\min,\text{amb}}/(g\cdot\text{fit})} - \frac{\left(g - \frac{g_{\min,\text{cas}}}{g\cdot\text{fit}}\right)\left(\frac{C_{\text{cas}}}{(MIC_S\cdot CS_{\text{amb}-\text{cas}})}\right)^{H_{\text{cas}}}}{\left(\frac{C_{\text{cas}}}{(MIC_S\cdot CS_{\text{amb}-\text{cas}})}\right)^{H_{\text{cas}}} - g_{\min,\text{cas}}/(g\cdot\text{fit})},$$

$$D_{\text{eff}}\left(R_{\text{cas}}\right) = 1 - \frac{\left(g - \frac{g_{\min,\text{amb}}}{g}\right)\left(\frac{C_{\text{amb}}}{(MIC_S\cdot CS_{\text{cas}-\text{amb}})}\right)^{H_{\text{amb}}}}{\left(\frac{C_{\text{amb}}}{(MIC_S\cdot CS_{\text{cas}-\text{amb}})}\right)^{H_{\text{amb}}} - g_{\min,\text{amb}}/g} - \frac{\left(g - \frac{g_{\min,\text{cas}}}{g}\right)\left(\frac{C_{\text{cas}}}{MIC_{\text{cas}}}\right)^{H_{\text{cas}}}}{\left(\frac{C_{\text{cas}}}{MIC_{\text{cas}}}\right)^{H_{\text{cas}}} - g_{\min,\text{cas}}/g}.$$

We assumed the drug effects of amphotericin B and caspofungin to be additive. The second and last terms represent the drug effect represent of AMB and CAS respectively. To determine the threshold drug concentration preventing growth, we introduced the terms ***MIC$_S$, MIC$_{amb}$*** and ***MIC$_{cas}$*** (expressed as ***MIC$_{50}$***) which stand for the minimum inhibitory concentrations for the parental, amphotericin B- and caspofungin-resistant strains, respectively. Collateral sensitivity is incorporated by the term ***CS*** (with range 0-1) and determines the increased sensitivity to the antifungal by altering the MIC. The Hill coefficient, which captures the steepness of the antifungal inhibition curve, is represented by the term ***H(amb – cas)***. Within the context of drug treatment, ***g_{min}*** is a parameters representing the minimum growth rate (death rate) in the presence of the drugs.

A. General modelling approach

We built upon the model proposed by Aulin *et al.*[20] to tailor the model to our specific system. We did this by incorporating specific pharmacokinetics of amphotericin B and caspofungin (based on clinically relevant doses and half-lives, see below for details), implementing the empirically derived collateral sensitivity value, and altering g_{min} to obtain realistic killing effects of each drug. While we drew on insights from *in vitro* data in the modelling approach, it is important to stress that these insights acted as guiding posts rather than direct quantitative inputs. For instance, the base model predicted extinction for some drug concentrations whereas the *in vitro* experiments did not. To ensure that the model arrives at conservative estimates of population extinction, we adjusted the drug killing potency g_{min}, in line with the empirical data (**Table S4** and **Table S5, Supplementary**). This same correction factor was then used for the *in vivo* model to ensure that the estimates of extinction were conservative (see below for details). Overall, the modelling outcomes should not be taken as quantitative predictions but rather as qualitative hypotheses that can be empirically tested. The justification of chosen parameter value is in the following and in **Table S10 (Supplementary).**

B. Drug specific parameters

We assumed daily administration of amphotericin B and caspofungin at 1.25 µg/ml and 6 µg/ml respectively, conform clinically relevant dose administration that result in a maximum concentration (C_{max}) of 2.1 µg/ml and 7 µg/ml[104]. We assumed mono-exponential decay of drugs and implemented it as follows:

$$\frac{dA_{\mathrm{D}_i}}{dt} = -k_{\mathrm{e,D_i}} \times A_{\mathrm{D}_i}$$

$$t_{\mathrm{half,\ D}_i} = \frac{\ln(2)}{k_{\mathrm{e,D}_i}}$$

These pharmacokinetic parameters were used to adjust the drug concentrations in the ODE model over time. g_{min} for amphotericin B was set at -2, representing a fungicidal effect, while for caspofungin, g_{min} was set at -0.5 and as it acts fungistatically. These values were obtained by comparing *in vitro* modelling with empirical data from experiments and based on literature[104,105]. In particular, the maximum killing capacity of the drugs was chosen to account for reduced drug efficacy, ensuring that the model makes conservative predictions of population extinction. These parameter values in the model resulted in population extinction with no resistance development only at high drug concentration (3xMIC). However, changing g_{min} estimates within a reasonable value range does not significantly affect the qualitative result of the cycling treatment as long as there is a significant difference in g_{min} between the two drugs. The g_{min} for amphotericin B is hard to estimate from literature, especially for the *in vivo* scenario. For caspofungin the relatively mild fungistatic effect is estimated from the *in vitro* data as even at high concentrations the drug does not result in population extinction (**Figure S1,** Supplementary).The Hill coefficient of amphotericin B and caspofungin were set to 4 and 1 respectively, based on *in vitro* dose response curves (**Figure S1,** Supplementary) and literature[105,106]. In particular, the g_{min} for amphotericin B was in accordance with the literature[105,106] and left unchanged, for caspofungin a direct estimate could not be found in the literature but *in vitro* data was sufficient to estimate its effect on growth since even at high concentrations the drug does not result in population extinction (**Figure S1,** Supplementary).

C. Drug resistance parameters

Resistance evolution was included as a stochastic mutation process with a mutation probability equal to a mutation rate (μ) of 10^{-8} as measured empirically. The number of cells mutated depended on the number of cells available (population size) per time step. Resistance was integrated as relative MIC change based on median values of 6 tested adaptors: with caspofungin resistance leading to a 32-fold increase in MIC and amphotericin B resistance leading to a 3-fold increase in MIC. The empirically estimated median collateral sensitivity of amphotericin B-resistant cells to caspofungin and vice versa was 0.5 (**Table S3, Supplementary**).

D. Population parameters

The size of the initial infecting population was set to 10^7 cells/ml. The growth rate of the parental strain was measured as 0.19 h^{-1} which translates to 3.6 cell divisions/h. The relative fitness cost of resistant cells was derived from the median change in growth rate of 6 tested resistant adaptors and measured to be 0.97, which was assumed to be not conferring a significant effect on fitness and therefore set to 1 for caspofungin-resistant adaptors. For amphotericin B-resistant adaptors the median relative growth rate compared to the parental strain was 0.79 (decreased with 21%) which is the **fit** value. The maximum carrying capacity

was 10^8 cells in the reservoir however, because of the immune system mediated killing, the effective carrying capacity was lower in simulations.

E. Immune killing parameters

The model includes the effect of the immune mediated killing of *C. auris* cells during infection, specifically focusing on a population of polymorphonuclear neutrophilic granulocytes (PMN). This is implemented as follows:

$$\frac{dE}{dt} = q\,(e_{\max} - E) - lE$$

We incorporated the action of a pathogen density-independent innate immune response symbolized by *E(t)*. PMN cells are drawn to the infection site at a rate defined by the equation $q \times (e_{max} - E(t))$, where q is a constant proportional to their recruitment speed and e_{max} represents the total density of effector cells in the reservoir[107,108]. Upon reaching the site of infection, the PMNs undergo inactivation at a consistent rate *l.* The killing efficiency of these immune cells corresponds directly to their density. This immune mediated killing rate is represented by the parameter j_n. The fungal cell killing rate was parameterized considering a healthy patient with a PMN count of 10^6 as the starting condition, in which infection would self-clear within 24 hours (both sensitive and resistant subpopulation would go extinct). This parameter estimate ($J_n = 5\text{x}10^{-6.5}$) is in accordance with blood infection dynamics of *Candida albicans,* where a PMN count of 10^6 leads to a 10-fold decrease in fugal population within 4 hours[107]. The phagocytosis rate, or fungal cell killing rate, was scaled proportionately to the diminished PMN count in a neutropenic patient with 10^5 PMN/ml, based on Praußе *et al.*[108]. The overarching framework of the model is derived from the model of Ankomah and Levin[109] used for understanding bacteria and other pathogens (e.g. Kochin *et al.*[110]) and was specifically applied here for *C. auris* systemic infections, incorporating the action of a pathogen density-independent innate immune response.

Plasmids and cloning

The SAT1 flipper previously optimized for *C. albicans* (pSFS2)[111] was used as a template to construct a linear cassette containing a dominant nourseothricin (NTC) resistance marker (*NAT*) flanked by the sequence of the CauNEUT locus. The CauNEUT was split in an upstream and a downstream element, with length of 267 bp and 271 bp respectively. The two elements were amplified by PCR using the primers D-5489 and D-5483 (upstream) and D-5485 and D-5486 (downstream), as listed in **Table S8** (Supplementary). The resistance marker was amplified by PCR using the primers D-5484 and D-5490 (**Table S8**, Supplementary). The resistance cassette was assembled by combining the products of the 3 amplicons in equimolar concentrations and performing a final PCR using the primers D-5486 and D-5489 (**Table S8**, Supplementary). PCR was performed by initial denaturation of 30sec. at 98°C, 30 cycles of 15sec. at 98°C, 30sec. at the primer specific annealing temperature, 30sec. per kb at 72°C and a final extension for 2 min. at 72°C. The annealing temperature was calculated by Tm Calculator (NEB) for every primer pair and Q5 polymerase (NEB) was used as the polymerase enzyme. PCR products were

purified from a 1% agarose (Eurogentec) gel, using the NucleoSpin Gel and PCR Clean-up XS kit (MN).

Strain construction

To construct the wt^{NAT} knock-in strain, a single colony of the B8441 isolate (wild type) was inoculated in liquid YPD and grown overnight at 37 °C, shaking at 220 rpm. This preculture was diluted in 50 mL YPD in a conical flask to an OD_{600} of 0.4 and grown until the OD_{600} reached a range of 1.6 to 2.2 (approximately 3-4 hours). The cells were collected by centrifugation (5 min. at 3,273xg) decanting supernatant and resuspension in 10 mL of transformation buffer [10 mM Tris-HCl, 1 mM EDTA-Na_2 (VWR) and 100 mM LiOAc (Sigma)]. This mixture was incubated at 37°C, shaking at 220 rpm. for 1 hour, after which 250 mL of 1M DTT (VWR) was added, following incubation for another 30 min. Next, cells were washed by centrifugation (5 min. at 5,000xg), decanting supernatant and resuspension in 25 mL ice-cold dH_2O, after which cells were washed with the same procedure in 5 mL ice-cold 1 M sorbitol (Sigma). Finally, cells were pelleted, the supernatant was removed carefully, and the pellet was resuspended in 200 mL of ice-cold 1 M sorbitol. 40 mL of these competent cells were mixed with the transformation mixture and transferred in a 2 mm electroporation cuvette (Pulsestar, Westburg). The transformation mixture comprised 3 µL of 4 mM Alt-R™ S.p. Cas9 Nuclease V3, 3.6 µL of duplexed sequence-specific Alt-R® CRISPR-Cas9 crRNA (IDT) with Alt-R® CRISPR-Cas9 tracrRNA (IDT) and 500 ng of the resistance cassette as dDNA. The sequence of the crRNA is shown in **Table S8** (Supplementary).

A single pulse was given at 1.8 kV, 200 Ω, 25 µF, and the transformation mixture was transferred to 2 mL YPD in a glass tube following incubation for 4 hours at 37°C, shaken at 220 rpm. The cells were collected by centrifugation at 5,000xg for 5 min., resuspended in 100 mL YPD and plated on YPD agar containing 200 mg/mL of nourseothricin (Jena bioscience). Colonies appeared after two days of incubation at 37°C. Correct transformants were identified by screening colonies with colony PCRs, using the Taq DNA Polymerase (NEB) and primers D-5487 and D-5488. Successful integration was confirmed by sequencing (Mix2Seq, Eurofins Genomics) of the PCR amplicon using primers D-5487 and D-5488 (**Table S8,** Supplementary).

Phenotyping of CauNEUT

To assess whether the integration of the SAT1 cassette in the CauNEUT had an effect on the strain phenotype, we evaluated two NAT-tagged knock-in transformants (further referred to as wt^{NAT_A} and wt^{NAT_B}) and the wild type strain for differential susceptibility for different stressors (see *A)* and antifungal agents (see *Drug susceptibility testing)* and differential growth in various conditions (see *B*).

A. Stress susceptibility testing

We evaluated susceptibility to eight stressors: cell wall stressors caffeine (CAF), calcofluor white (CFW) and Congo red (CR), membrane stressor sodium dodecyl sulphate (SDS), oxidative stressors hydrogen peroxide (H_2O_2) and dipropylenetriamine NONOate (DPTA NONOate), osmotic stressor sodium chloride (NaCl) and bivalent cation chelator ethylenediaminetetraacetic acid (EDTA). Stress susceptibility was assessed by broth dilution

assay similar to drug susceptibility testing. Briefly, a 2-fold dilution range of stressor was prepared in a final volume of 200 µL RPMI-MOPS (pH 7, 2% glucose) medium with 100-500 cells (based on OD_{600nm} and serial dilution) was seeded in a round-bottom 96-well polystyrene microtiter plate (Greiner). Plates were incubated at 37°C for 48 hours, and growth was assessed spectrophotometrically (OD_{600}) using a Synergy™ H1 microplate reader (BioTek). Stressor dilution ranges were 10 - 0.04 mM for H_2O_2 (Sigma-Aldrich), 10 - 0.04 mM for CFW (Fluorescent Brightener 28, Sigma-Aldrich), 12 - 0.05 µM for CR (Sigma-Aldrich), 2.5 - 0.01 M for NaCl (Sigma-Aldrich), 3.47 - 0.014 mM for SDS (Sigma-Aldrich), 7.5 – 0.03 mM for DPTA NONOate (Sigma-Aldrich), 52.5 – 0.21 mM for CAF (Sigma-Aldrich) and 2 - 0.0078 mM for EDTA (VWR) in the final volume of the broth dilution assay. Each strain was tested in duplicate (technical repeats) for each stressor.

B. Growth analyses

We evaluated growth conform the method described in *Growth analysis*, but with variations in glucose concentration (0.2% and 2%), incubation temperature (37°C and 41°C) and pH (pH4, 7 and 8) or the addition of NaCl (1M), H_2O_2 (2.5 µM), CR (2.87 µM), CFW (520 µM) or SDS (173.38 µM). The medium was buffered with 50 mM Citrate buffer for pH4 and 100 mM MOPS buffer for pH 7 and 8. All cultures were diluted in 200 µL RPMI-MOPS to a final cell concentration of 10^6 cells per well in a flat-bottom 96-well microtiter plate (Greiner). Growth was monitored spectrophotometrically for 72h at OD_{600} in a Multiskan GO automated plate reader (Thermo Scientific) with intermittent (10 min. interval) pulsed (1 min medium strength) shaking and 30-minute interval measurements.

Competitive fitness experiments

Competitive fitness experiments were carried out in 200 µL RPMI-MOPS (2% glucose) with a final cell concentration of 10^6 cells per well in a round-bottom 96-well microtiter plate (Greiner). The resistant adaptor of interest and wt^{NAT_A} strain were separately grown overnight and mixed in a 50:50 ratio at time point 0. The drugs tested were amphotericin B, caspofungin and flucytosine, evaluated at concentrations of 1xMIC_{50} values of the wt strain (**Table 1**). Plates were incubated at 37°C and populations were 1/10 diluted (20 µL transfer to 180 µL fresh medium at 37°C) every 48h. The relative population size of resistant and wt^{NAT_A} cells was assessed by plating on YPD and colony replicating using a velvet replicator on YPD + 100mg/l NTC at 0 (after mixing), 48h, 96h, 144h, and 192h post inoculation. To ensure CFU enumeration within the countable range (10-200 CFUs), cultures were diluted in PBS prior to plating, based on relative total population size estimated spectrophotometrically (OD_{600}) using a Synergy™ H1 microplate reader (BioTek). The relative subpopulation proportion of resistant cells was estimated by extracting CFU count on YPD + NTC (wt^{NAT}) plates from total CFU count in YPD plates. All microtiter plates were stored at -80°C after addition of glycerol to a final concentration of 27% per well.

Whole genome sequencing and analysis

Adaptors 1 and 2 were sequenced on an Illumina NovaSeq6000 platform, while the sequences from adaptor 3-19 and all 4 parental wild type strains were retrieved from NCBI (accession numbers are displayed in **Table S9,** Supplementary).

Variant calling analysis was performed using the perSVade suite (version 1.0.6), a comprehensive set of tools tailored for sequencing read trimming, quality assessment, alignment, variant detection, and the annotation of identified variants[112]. To remove adaptors and trim the reads for each sample, we used FastQC (v. 0.11.9)[113] and Trimmomatic (v. 0.38)[114] with default parameters, facilitated by the trim_reads_and_QC module of perSVade (v. 1.02.6). This was followed by alignment of the trimmed reads (with BWA MEM (v. 0.7.17) to the *Candida auris* B8441 reference genome (v. s01-m01-r27), available on the Candida Genome Database (CGD), using the align_reads module of perSVade (v. 1.02.6).

Next, using perSVade (v. 1.02.6 module call_small_variants) we performed variant calling on the aligned reads and functional annotation of small variants (SNPs and small indels). The results integrate output from three different variant callers: BCFtools (v. 1.9)[115], GATK Haplotype Caller (v. 4.1.2)[116], and Freebayes (v. 1.3.1)[117]. For variant calling, we set the '–ploidy 1' option, under the assumption that the canonical ploidy is consistent across all the strains. For adaptors 2-18 and parental wild type strains, haploidy was confirmed in Carolus *et al.*[50] . Variants with coverage below 30 and a minimum fraction of reads covering a variant (--min_AF) below 0.9 were filtered out. Moreover, obtained variants were filtered to retain only those that passed the stringent filters of all three calling tools, ensuring a collection of high-confidence variants per sample. Variants identified in parental wild type strains were removed from the high-confidence sets (with BCFtools v. 1.15.1[115] function isec) to distinguish mutations associated with evolutionary adaptations of adaptors from the background genetic variation.The annotation of newly acquired variants for each adaptor was performed with perSVade v. 1.02.6, (annotate_small_vars module with Ensembl Variant Effect Predictor v. 100.2[118]). For correct functional annotation, we used NCBI Table 12 and Table 3 (https://www.ncbi.nlm.nih.gov/Taxonomy/Utils/wprintgc.cgi) for Genetic and Mitochondrial Genetic code translation, respectively. Given that the *C. auris* B8441 reference genome does not include mitochondrial DNA annotations, the study was limited to variants present in nuclear chromosomes.

To optimize sequencing data analysis we used the run_several_modules feature from perSVade v1.03.1 (yet to be released), but it is worth noting that the core functionality mirrors that of perSVade v1.02.6 release (program versions for trimming, quality control, alignment, variant calling and annotation are the same).

Structural variants such as spanning deletions or chromosomal duplications were not investigated in this study. Information on structural variants reported in **Table S9** (Supplementary) are taken from Carolus *et al.*[50]

Data availability

C. auris strains are available per request or via the CDC & FDA Antibiotic Resistance Isolate Bank (https://wwwn.cdc.gov/arisolatebank/; panel ID CAU). Illumina sequencing output is available via the NCBI sequence read archive (SRA), BioProject PRJNA1096176 (this study) accession numbers SRR28553515-SRR28553516, BioProject PRJNA984918[50] accession numbers SRR26533547-SRR26533554; SRR26533558; SRR26533563; SRR26533567-SRR26533570; SRR26533573 and SRR26533574, and BioProject PRJNA664007[52] accession numbers SRR12659405 and SRR12659402 (see **Table S9,** Supplementary for strain info). Further information or requests should be directed to and will be fulfilled by the lead contacts: Hans Carolus (hans.carolus@kuleuven.be) and Patrick Van Dijck (patrick.vandijck@kuleuven.be).

Code availability

The code used for mathematical modelling is available via GitHub: https://github.com/GiorgioBoccarella/cs_paper_model.git

Acknowledgments

This work is part of the CycleDrug project, which has been supported by the Fund for Scientific Research Flanders (FWO) under the framework of the JPIAMR – Joint Programming Initiative on Antimicrobial Resistance fund (G0L1622N), granted to P.V.D., T.G., J.B. and K.L. Additionally, this work was supported by a C3 grant from the Industrial Research Fund of KU Leuven (C3/22/007) granted to P.V.D. and K.L. Researchers H.C., D.S., S.J. and G.B. were supported by FWO PhD fellowships 11D7620N, 11J8122N, 11PRR24N and 1150023N respectively. H.C. was also supported by a post-doctoral fellowship granted by KU Leuven Internal Funds (PDMT2/23/032). V.B. received funding from the European Union's Horizon 2020 research and innovation programme under the Marie Skłodowska-Curie grant agreement No 945352. The T.G. group acknowledges support from the Spanish Ministry of Science and Innovation (grant numbers PID2021-126067NB-I00, CPP2021-008552, PCI2022-135066-2, and PDC2022-133266-I00), cofounded by ERDF "A way of making Europe", as well as support from the Catalan Research Agency (AGAUR) (grant number SGR01551); "La Caixa" foundation (grant number LCF/PR/HR21/00737), and Instituto de Salud Carlos III (IMPACT grant IMP/00019 and CIBERINFEC CB21/13/00061- ISCIII-SGEFI/ERDF). J.B. was also supported by funding from the European Research Council (ERC) under the European Union's Horizon 2020 research and innovation program (grant agreement No 951475, ERC SYN FungalTolerance), by the Israel Science Foundation (award #997/18) and the Israeli Ministry of Science Technology & Space (award #88555). P.v.d.B acknowledges the support of KU Leuven start-up funding (GNM-E1097-STG/21/003).

Author contributions

H.C. conceptualized, designed and supervised the study, provided funding, carried out experiments, data analysis and wrote the manuscript. D.S. and S.J. carried out experiments and data analysis and provided conceptual insights. G.B. designed and carried out mathematical modelling. V.B. carried out WGS data analysis. L.G., A.C., I.V. and T.V. carried out experiments. S.P. and H.S. provided conceptual insights. P.v.d.B. supervised mathematical

modelling. K.L., T.G., J.B. and P.V.D. provided funding and supervised the study. All authors edited and approved the manuscript.

Competing interests

The authors declare no competing interests.

Table 1: Drugs used in this study and parental strain susceptibility. Drugs are listed per drug class/type. MIC_{50}: minimum inhibitory concentration of 50% growth in a Broth Dilution Assay (BDA in µg/ml). AUC: area under the BDA growth – vs – drug concentration curve (in µg/ml*$\%_{growth}$). All drugs were tested in a 2-fold dilution range from 16 µg/ml to 0.0625 µg/ml of drug and compared to a drug-free control. Effect indicates whether the drugs showed fungistatic or fungicidal effect within that tested range: drugs are termed fungicidal when there is <99% survival of cells in at least one concentration in the BDA. The MFC: minimum fungicidal (<99% survival) concentration (in µg/ml), is assessed by spot replicating BDA plates on agar. The drugs used for experimental evolution in single-drug administration are displayed in italics. Dose-response profiles are shown **Figure S1 (**Supplementary)**.**

Figure 1: Experimental evolution of drug resistance followed by drug susceptibility testing **A)** Schematic representation of experimental evolution, adaptor selection and susceptibility screening as described in *Methods*. Top panels from left to right: A single wild type (wt) parental strain was used to evolve resistance in 9 drugs, 4 concentrations each for 7 passages over 14 days. Next, 6 independent resistant adaptors for each drug were tested for CS (RR<1) or XR (RR>1) to 18 different drugs. **B)** Relative drug susceptibility of max. 24 independently evolved adaptors per drug. Red lines indicate median values. Symbol shape indicates drug dose in which adaptors evolved as indicated in legend. Significant differences based on non-parametric one-way ANOVA are shown by asterisks (*p-value<0.05; **p-value<0.01; ***p-value<0.001; ****p-value<0.0001). Test details see **Table S11** (Supplementary). Values and MIC_{50} data see **Table S1** and **Figure S2A (**Supplementary) resp. **C)** CS/XR heatmap based on RR(AUC). Rows represent 6 resistant [RR(AUC)>1] adaptors per drug and columns represent tested drugs. Blue indicates CS (RR<1), orange indicates XR (RR>1). Values and MIC_{50} data are provided in **Table S2-3** and **Figure S2B** (Supplementary) resp. Drug abbreviations and parental strain susceptibility are listed in **Table 1** and **Table S1** (Supplementary) resp. Resistance ratio [RR(AUC) = AUC (evolved adaptor)/AUC (parental strain)] with AUC: area under the growth – vs – drug concentration curve of the broth dilution assay (BDA). Panel A) was created with BioRender.com

Figure 2: Distribution of MIC_{50} values for non-conventional antifungal agents of all isolates evolved in single drug exposure (isolates shown in **Figure 1C**). The MIC_{50} values displayed are shown in **Table S3** (Supplementary). The black diamond symbol represents the parental wt strain MIC_{50} value for each drug. Drug abbreviations see **Table 1.**

Figure 3: Resistance evolution in CS-based therapy versus single drug regimens. Resistance development of individual adaptors isolated from *in vitro* experimental evolution in single drug exposure compared to 4-day drug cycling or combined administration of three different CS-drug pairs **(A)** and one XR-drug pair **(B)**. Boxes indicate 25th to 75th percentile with line at median and whiskers indicate minimum and maximum range. The colour of the box indicates which drug is tested and the symbol indicates in which drug dose combination the adaptors were evolved, as indicated in the legend. In cyclic (/) and combined (+) administration, 4 dose combinations are used, with L= 1xMIC_{50} and H=2xMIC_{50} (except for GEL and 5FC, see *Methods*). The order of dose combinations can be inferred from the treatment description on the x-axis (e.g. AMB/GEL - LH means low AMB and high GEL). Values and MIC_{50} data see **Table S4** and **Figure S3** (Supplementary) resp. Statistical pairwise comparisons consist of single drug vs cycling, single drug vs combination therapy, and cyclic vs combination therapy. **C)** Model prediction of resistant and susceptible sub-population sizes after 8 days of

monotherapy, daily, 2-day and 4-day drug cycling of AMB and CAS, based on 100 simulations. Values see **Table S6** (Supplementary). **D)** A single model simulation of population dynamics of susceptible (wt), AMB-resistant (AMB-R), CAS-resistant (CAS-R) and immune effector cells in the upper graph and drug pharmacokinetics in lower graph, during AMB monotherapy (solid lines) and daily drug cycling of AMB and CAS (dotted lines). Significant differences based on non-parametric one-way ANOVA are shown by asterisks (*p-value<0.05; **p-value<0.01; ***p-value<0.001; ****p-value<0.0001). Test details see **Table S11** (Supplementary).

Figure 4: Competitive fitness of amphotericin B-resistant adaptors vs parental susceptible cells in different treatment conditions. Six AMB-resistant adaptors (dark green symbols) were individually mixed in 50:50 ratios with the wt^{NAT} strain (dark pink symbols), and serially diluted (1/10) into fresh medium every 48h (conform the *in vitro* experimental evolution assay) for 8 days. Relative population size of the AMB-resistant and susceptible cells was estimated every 48h by selective plating on YPD agar and replication of colonies on YPD agar supplemented with NTC. The mean relative population size of two experimental (technical) repeats per adaptor mixture is shown by coloured symbols. Different strain mixtures are represented by different symbol shapes that represent the same AMB-resistant adaptor in all graphs. Values see **Table S7** (Supplementary). Barplots (light green and pink) and black error bars represent the mean and SEM of all averaged proportions per time point in each condition. Population dynamics over time is shown in absence of drug **(A)** and during administration of $1xMIC_{50}$ AMB (**B)**, $1xMIC_{50}$ CAS (**C)** and $1xMIC_{50}$ 5FC (**D)**, with drug concentrations relative to the parental wt MIC_{50} (**Table 1**).

Figure 5: XR/CS map and genotype of amphotericin B-resistant adaptors from 4 clades. CS/XR heatmap based on RR(AUC). Rows represent 6 amphotericin B-resistant [RR(AUC)>1] adaptors from Clade I (adaptor 1-6; same adaptors as shown in **Figure 1C** and competitive fitness experiments **Figure 4**), Clade III (adaptor 7-12), Clade IV (adaptor 13-18) and Clade II (adaptor 19). Columns represent tested drugs. Blue indicates CS (RR<1), orange indicates XR (RR>1). MIC_{50} data see **Figure S8** (Supplementary). 'variant *ERG* gene' indicates which gene involved in ergosterol biosynthesis holds a resistance-conferring mutation, 'variant' indicates which mutation in the respective '*ERG* genes' was identified. Full variant calling output is displayed in **Table S9** (Supplementary). Drug abbreviations and parental strain susceptibility see **Table 1**, **Figure S1** and **Figure S9** (Supplementary).

References

1 Denning, D. W. Global incidence and mortality of severe fungal disease. *The Lancet Infectious Diseases* **24**, E428-E438 (2024). https://doi.org:10.1016/S1473-3099(24)00103-8

2 Almeida, F., Rodrigues, M. L. & Coelho, C. The Still Underestimated Problem of Fungal Diseases Worldwide. *Frontiers in Microbiology* **10** (2019). https://doi.org:10.3389/fmicb.2019.00214

3 Fisher, M. C. & Denning, D. W. The WHO fungal priority pathogens list as a game-changer. *Nature Reviews Microbiology* **21**, 211–212 (2023). https://doi.org:10.1038/s41579-023-00861-x

4 Jermy, A. Stop neglecting fungi. *Nature Microbiology* **2**, 17120 (2017). https://doi.org:10.1038/nmicrobiol.2017.120

5 Perfect, J. R. The antifungal pipeline: a reality check. *Nature Reviews Drug Discovery* **16**, 603-616 (2017). https://doi.org:10.1038/nrd.2017.46

6 Lockhart, S. R., Chowdhary, A. & Gold, J. A. W. The rapid emergence of antifungal-resistant human-pathogenic fungi. *Nature Reviews Microbiology* **21**, 818–832 (2023). https://doi.org:10.1038/s41579-023-00960-9

7 Fisher, M. C., Hawkins, N. J., Sanglard, D. & Gurr, S. J. Worldwide emergence of resistance to antifungal drugs challenges human health and food security. *Science* **360**, 739-742 (2018). https://doi.org:10.1126/science.aap7999

8 Satoh, K. *et al. Candida auris* sp. nov., a novel ascomycetous yeast isolated from the external ear canal of an inpatient in a Japanese hospital. *Microbiology and Immunology* **53**, 41-44 (2009). https://doi.org:10.1111/j.1348-0421.2008.00083.x

9 Lockhart, S. R. *et al.* Simultaneous emergence of multidrug-resistant *Candida auris* on 3 continents confirmed by whole-genome sequencing and epidemiological analyses. *Clinical Infectious Diseases* **64**, 134-140 (2017). https://doi.org:10.1093/cid/ciw691

10 Rhodes, J. & Fisher, M. C. Global epidemiology of emerging *Candida auris*. *Current Opinion in Microbiology* **52**, 84-89 (2019). https://doi.org:10.1016/j.mib.2019.05.008

11 CDC. *Antibiotic resistance threats in the United States*, <https://www.cdc.gov/drugresistance/biggest-threats.html> (2019).

12 Rybak, J. M., Cuomo, C. A. & David Rogers, P. The molecular and genetic basis of antifungal resistance in the emerging fungal pathogen *Candida auris*. *Current Opinion in Microbiology* **70**, 102208 (2022). https://doi.org:10.1016/j.mib.2022.102208

13 Imamovic, L. & Sommer, M. O. Use of collateral sensitivity networks to design drug cycling protocols that avoid resistance development. *Science Translational Medicine* **5**, 204ra132 (2013). https://doi.org:10.1126/scitranslmed.3006609

14 Munck, C., Gumpert, H. K., Wallin, A. I., Wang, H. H. & Sommer, M. O. Prediction of resistance development against drug combinations by collateral responses to component drugs. *Science Translational Medicine* **6**, 262ra156 (2014). https://doi.org:10.1126/scitranslmed.3009940

15 Pal, C., Papp, B. & Lazar, V. Collateral sensitivity of antibiotic-resistant microbes. *Trends in Microbiology* **23**, 401-407 (2015). https://doi.org:10.1016/j.tim.2015.02.009

16 Pluchino, K. M., Hall, M. D., Goldsborough, A. S., Callaghan, R. & Gottesman, M. M. Collateral sensitivity as a strategy against cancer multidrug resistance. *Drug Resistance Updates* **15**, 98-105 (2012). https://doi.org:10.1016/j.drup.2012.03.002

17 Hall, M. D., Handley, M. D. & Gottesman, M. M. Is resistance useless? Multidrug resistance and collateral sensitivity. *Trends in Pharmacological Sciences* **30**, 546-556 (2009). https://doi.org:10.1016/j.tips.2009.07.003

18 Szybalski, W. & Bryson, V. Genetic studies on microbial cross resistance to toxic agents I. Cross resistance of *Escherichia coli* to fifteen antibiotics. *Journal of Bacteriology* **64**, 489-499 (1952). https://doi.org:10.1128/jb.64.4.489-499.1952

19 Kim, S., Lieberman, T. D. & Kishony, R. Alternating antibiotic treatments constrain evolutionary paths to multidrug resistance. *PNAS* **111**, 14494-14499 (2014). https://doi.org:10.1073/pnas.1409800111

20 Aulin, L. B. S., Liakopoulos, A., van der Graaf, P. H., Rozen, D. E. & van Hasselt, J. G. C. Design principles of collateral sensitivity-based dosing strategies. *Nature Communications* **12**, 5691 (2021). https://doi.org:10.1038/s41467-021-25927-3

21 Tetteh, J. N. A., Olaru, S., Crauel, H. & Hernandez-Vargas, E. A. Scheduling collateral sensitivity-based cycling therapies toward eradication of drug-resistant infections. *International Journal of Robust and Nonlinear Control* **33**, 4824-4842 (2023). https://doi.org:10.1002/rnc.6528

22 Maltas, J. & Wood, K. B. Pervasive and diverse collateral sensitivity profiles inform optimal strategies to limit antibiotic resistance. *PLOS Biology* **17**, e3000515 (2019). https://doi.org:10.1371/journal.pbio.3000515

23 Yen, P. & Papin, J. A. History of antibiotic adaptation influences microbial evolutionary dynamics during subsequent treatment. *PLOS Biology* **15**, e2001586 (2017). https://doi.org:10.1371/journal.pbio.2001586

24 Yoshida, M. *et al.* Time-programmable drug dosing allows the manipulation, suppression and reversal of antibiotic drug resistance *in vitro*. *Nature Communications* **8** (2017). https://doi.org:10.1038/ncomms15589

25 Barbosa, C., Römhild, R., Rosenstiel, P. & Schulenburg, H. Evolutionary stability of collateral sensitivity to antibiotics in the model pathogen *Pseudomonas aeruginosa*. *eLife* **8**, e51481 (2019). https://doi.org:10.7554/eLife.51481

26 Niederman, M. S. Appropriate use of antimicrobial agents: Challenges and strategies for improvement. *Critical care medicine* **31** (2003). https://doi.org:10.1097/01.CCM.0000050464.70382.D6

27 Brepoels, P. *et al.* Antibiotic Cycling Affects Resistance Evolution Independently of Collateral Sensitivity. *Molecular Biology and Evolution* **39**, msac257 (2022). https://doi.org:10.1093/molbev/msac257

28 Lukens, A. K. *et al.* Harnessing evolutionary fitness in *Plasmodium falciparum* for drug discovery and suppressing resistance. *PNAS* **111**, 799-804 (2014). https://doi.org:10.1073/pnas.1320886110

29 Rodriguez de Evgrafov, M., Gumpert, H., Munck, C., Thomsen, T. T. & Sommer, M. O. A. Collateral Resistance and Sensitivity Modulate Evolution of High-Level Resistance to Drug Combination Treatment in *Staphylococcus aureus*. *Molecular Biology and Evolution* **32**, 1175-1185 (2015). https://doi.org:10.1093/molbev/msv006

30 Rosenkilde, C. E. H. *et al.* Collateral sensitivity constrains resistance evolution of the CTX-M-15 β-lactamase. *Nature Communications* **10**, 618 (2019). https://doi.org:10.1038/s41467-019-08529-y

31 Dromer, F., Bernede-Bauduin, C., Guillemot, D. & Lortholary, O. Major Role for Amphotericin B–Flucytosine Combination in Severe Cryptococcosis. *PLOS ONE* **3**, e2870 (2008). https://doi.org:10.1371/journal.pone.0002870

32 Maziarz, E. K. & Perfect, J. R. in *Diagnosis and Treatment of Fungal Infections* (eds Duane R. Hospenthal, Michael G. Rinaldi, & Thomas J. Walsh) 245-265 (Springer International Publishing, 2023).

33 Pappas, P. G. *et al.* Clinical Practice Guideline for the Management of Candidiasis: 2016 Update by the Infectious Diseases Society of America. *Clinical Infectious Diseases* **62**, e1-50 (2016). https://doi.org:10.1093/cid/civ933

34 Aghaei Gharehbolagh, S. *et al.* New weapons to fight a new enemy: A systematic review of drug combinations against the drug-resistant fungus *Candida auris*. *Mycoses* **64**, 1308-1316 (2021). https://doi.org:10.1111/myc.13277

35 Hill, J. A., O'Meara, T. R. & Cowen, L. E. Fitness Trade-Offs Associated with the Evolution of Resistance to Antifungal Drug Combinations. *Cell Reports* **10**, 809-819 (2015). https://doi.org:10.1016/j.celrep.2015.01.009

36 Maertens, J. A. History of the development of azole derivatives. *Clinical Microbiology and Infection* **10**, 1-10 (2004). https://doi.org:10.1111/j.1470-9465.2004.00841.x

37 Szymański, M., Chmielewska, S., Czyżewska, U., Malinowska, M. & Tylicki, A. Echinocandins - structure, mechanism of action and use in antifungal therapy. *Journal of Enzyme Inhibition and Medicinal Chemistry* **37**, 876-894 (2022). https://doi.org:10.1080/14756366.2022.2050224

38 Stevens David, A., Espiritu, M. & Parmar, R. Paradoxical Effect of Caspofungin: Reduced Activity against *Candida albicans* at High Drug Concentrations. *Antimicrobial Agents and Chemotherapy* **48**, 3407-3411 (2004). https://doi.org:10.1128/aac.48.9.3407-3411.2004

39 Kordalewska, M. *et al.* Understanding Echinocandin Resistance in the Emerging Pathogen *Candida auris*. *Antimicrobial Agents and Chemotherapy* **62**, aac.00238-00218 (2018). https://doi.org:10.1128/AAC.00238-18

40 Billamboz, M., Fatima, Z., Hameed, S. & Jawhara, S. Promising Drug Candidates and New Strategies for Fighting against the Emerging Superbug *Candida auris*. *Microorganisms* **9**, 634 (2021). https://doi.org:10.3390/microorganisms9030634

41 Bouz, G. & Doleal, M. Advances in Antifungal Drug Development: An Up-To-Date Mini Review. *Pharmaceuticals* **14**, 1312 (2021). https://doi.org:10.3390/ph14121312

42 Mamouei, Z. *et al.* Alexidine Dihydrochloride Has Broad-Spectrum Activities against Diverse Fungal Pathogens. *mSphere* **3** (2018). https://doi.org:10.1128/mSphere.00539-18

43 Berman, J. & Krysan, D. J. Drug resistance and tolerance in fungi. *Nature Reviews Microbiology* **18**, 319-331 (2020). https://doi.org:10.1038/s41579-019-0322-2

44 Petzoldt, T. *growthrates: Estimate Growth Rates from Experimental Data. R package version 0.8.4*, <https://CRAN.R-project.org/package=growthrates > (2022).

45 Gerami-Nejad, M., Zacchi, L. F., McClellan, M., Matter, K. & Berman, J. Shuttle vectors for facile gap repair cloning and integration into a neutral locus in *Candida albicans*. *Microbiology* **159**, 565-579 (2013). https://doi.org:10.1099/mic.0.064097-0

46 Kim, S. H. *et al.* Genetic Analysis of *Candida auris* Implicates Hsp90 in Morphogenesis and Azole Tolerance and Cdr1 in Azole Resistance. *mBio* **10** (2019). https://doi.org:10.1128/mBio.02529-18

47 Ko, H.-C., Hsiao, T.-Y., Chen, C.-T. & Yang, Y.-L. *Candida albicans ENO1* null mutants exhibit altered drug susceptibility, hyphal formation, and virulence. *Journal of Microbiology* **51**, 345-351 (2013). https://doi.org:10.1007/s12275-013-2577-z

48 Ennis, C. L., Hernday, A. D. & Nobile, C. J. A Markerless CRISPR-Mediated System for Genome Editing in *Candida auris* Reveals a Conserved Role for Cas5 in the Caspofungin Response. *Microbiology Spectrum* **9**, e01820-01821 (2021). https://doi.org:10.1128/Spectrum.01820-21

49 Santana, D. J. & O'Meara, T. R. Forward and reverse genetic dissection of morphogenesis identifies filament-competent *Candida auris* strains. *Nature Communications* **12**, 7197 (2021). https://doi.org:10.1038/s41467-021-27545-5

50 Carolus, H. *et al.* Acquired amphotericin B resistance and fitness trade-off compensation in *Candida auris*. *Research Square (preprint)* (2023). https://doi.org:10.21203/rs.3.rs-3621420/v1

51 Vincent, B. M., Lancaster, A. K., Scherz-Shouval, R., Whitesell, L. & Lindquist, S. Fitness Trade-offs Restrict the Evolution of Resistance to Amphotericin B. *PLOS Biology* **11**, e1001692 (2013). https://doi.org:10.1371/journal.pbio.1001692

52 Carolus, H. *et al.* Genome-Wide Analysis of Experimentally Evolved *Candida auris* Reveals Multiple Novel Mechanisms of Multidrug Resistance. *mBio* **12**, e03333-03320 (2021). https://doi.org:10.1128/mBio.03333-20

53 Carolus, H., Pierson, S., Lagrou, K. & Van Dijck, P. Amphotericin B and Other Polyenes-Discovery, Clinical Use, Mode of Action and Drug Resistance. *Journal of Fungi* **6**, 321 (2020). https://doi.org:10.3390/jof6040321

54 Barbosa, C. *et al.* Alternative Evolutionary Paths to Bacterial Antibiotic Resistance Cause Distinct Collateral Effects. *Molecular Biology and Evolution* **34**, 2229-2244 (2017). https://doi.org:10.1093/molbev/msx158

55 Kordalewska, M. *et al.* Rare modification in the ergosterol biosynthesis pathway leads to amphotericin B resistance in *Candida auris* clinical isolates. *bioRxiv (preprint)* (2021). https://doi.org:10.1101/2021.10.22.465535

56 Rybak, J. M. *et al.* *In vivo* emergence of high-level resistance during treatment reveals the first identified mechanism of amphotericin B resistance in *Candida auris*. *Clinical Microbiology and Infection* **28**, 838-843 (2022). https://doi.org:10.1016/j.cmi.2021.11.024

57 Chow, N. A. *et al.* Tracing the evolutionary history and global expansion of *Candida auris* using population genomic analyses. *mBio* **11** (2020). https://doi.org:10.1128/mBio.03364-19

58 Jeffery-Smith, A. *et al.* *Candida auris*: a Review of the Literature. *Clinical Microbiology Reviews* **31** (2017). https://doi.org:10.1128/CMR.00029-17

59 Després, P. C. *et al.* Asymmetrical dose responses shape the evolutionary trade-off between antifungal resistance and nutrient use. *Nature Ecology & Evolution* **6**, 1501-1515 (2022). https://doi.org:10.1038/s41559-022-01846-4

60 Wall, G., Herrera, N. & Lopez-Ribot, J. L. Repositionable Compounds with Antifungal Activity against Multidrug Resistant *Candida auris* Identified in the Medicines for Malaria Venture's Pathogen Box. *Journal of Fungi* **5**, 92 (2019). https://doi.org:10.3390/jof5040092

61 Subissi, A., Monti, D., Togni, G. & Mailland, F. Ciclopirox. *Drugs* **70**, 2133-2152 (2010). https://doi.org:10.2165/11538110-000000000-00000

62 Fuchs, F. *et al.* Antifungal activity of nitroxoline against *Candida auris* isolates. *Clinical Microbiology and Infection* **27**, 1697-1610 (2021). https://doi.org:10.1016/j.cmi.2021.06.035

63 Pristov, K. E. & Ghannoum, M. A. Resistance of *Candida* to azoles and echinocandins worldwide. *Clinical Microbiology and Infection* **25**, 792-798 (2019). https://doi.org:10.1016/j.cmi.2019.03.028

64 Panackal Anil, A. *et al.* Clinical Significance of Azole Antifungal Drug Cross-Resistance in *Candida glabrata*. *Journal of Clinical Microbiology* **44**, 1740-1743 (2006). https://doi.org:10.1128/jcm.44.5.1740-1743.2006

65 Forastiero, A. *et al.* *Candida tropicalis* Antifungal Cross-Resistance Is Related to Different Azole Target (Erg11p) Modifications. *Antimicrobial Agents and Chemotherapy* **57**, 4769-4781 (2013). https://doi.org:10.1128/aac.00477-13

66 Perlin, D. S. Resistance to echinocandin-class antifungal drugs. *Drug Resistance Updates* **10**, 121-130 (2007). https://doi.org:10.1016/j.drup.2007.04.002

67 Chassot, F. *et al.* Exploring the *In Vitro* Resistance of *Candida parapsilosis* to Echinocandins. *Mycopathologia* **181**, 663-670 (2016). https://doi.org:10.1007/s11046-016-0028-1

68 Arendrup, M. C. & Perlin, D. S. Echinocandin resistance: an emerging clinical problem? *Current Opinion in Infectious Diseases* **27**, 484-492 (2014). https://doi.org:10.1097/qco.0000000000000111

69 Kathuria, S. *et al.* Multidrug-Resistant *Candida auris* Misidentified as *Candida haemulonii*: Characterization by Matrix-Assisted Laser Desorption Ionization–Time of Flight Mass Spectrometry and DNA Sequencing and Its Antifungal Susceptibility Profile Variability by Vitek 2, CLSI Broth Microdilution, and Etest Method. *Journal of Clinical Microbiology* **53**, 1823-1830 (2015). https://doi.org:10.1128/jcm.00367-15

70 Arendrup, M. C., Prakash, A., Meletiadis, J., Sharma, C. & Chowdhary, A. Comparison of EUCAST and CLSI Reference Microdilution MICs of Eight Antifungal Compounds for *Candida auris* and Associated Tentative Epidemiological Cutoff Values. *Antimicrobial Agents and Chemotherapy* **61** (2017). https://doi.org:10.1128/AAC.00485-17

71 Sanglard, D., Ischer, F., Parkinson, T., Falconer, D. & Bille, J. *Candida albicans* mutations in the ergosterol biosynthetic pathway and resistance to several antifungal agents. *Antimicrobial Agents and Chemotherapy* **47**, 2404-2412 (2003). https://doi.org:10.1128/AAC.47.8.2404-2412.2003

72 Kelly, S. L. *et al.* Resistance to fluconazole and cross-resistance to amphotericin B in *Candida albicans* from AIDS patients caused by defective sterol Δ5, 6-desaturation. *FEBS letters* **400**, 80-82 (1997). https://doi.org:10.1016/S0014-5793(96)01360-9

73 Hull, C. M. *et al.* Facultative sterol uptake in an ergosterol-deficient clinical isolate of *Candida glabrata* harboring a missense mutation in *ERG11* and exhibiting cross-resistance to azoles and amphotericin B. *Antimicrobial Agents and Chemotherapy* **56**, 4223-4232 (2012). https://doi.org:10.1128/AAC.06253-11

74 Eddouzi, J. *et al.* Molecular mechanisms of drug resistance in clinical *Candida* species isolated from Tunisian hospitals. *Antimicrobial Agents and Chemotherapy* **57**, 3182-3193 (2013). https://doi.org:10.1128/AAC.00555-13
75 Rosenberg, A. *et al.* Antifungal tolerance is a subpopulation effect distinct from resistance and is associated with persistent candidemia. *Nature Communications* **9**, 2470 (2018). https://doi.org:10.1038/s41467-018-04926-x
76 Levinson, T. *et al.* Impact of tolerance to fluconazole on treatment response in *Candida albicans* bloodstream infection. *Mycoses* **64**, 78-85 (2021). https://doi.org:10.1111/myc.13191
77 Chen, L. *et al.* Brain glucose induces tolerance of *Cryptococcus neoformans* to amphotericin B during meningitis. *Nature Microbiology* **9**, 346-358 (2024). https://doi.org:10.1038/s41564-023-01561-1
78 Nichol, D. *et al.* Antibiotic collateral sensitivity is contingent on the repeatability of evolution. *Nature Communications* **10** (2019). https://doi.org:10.1038/s41467-018-08098-6
79 Yekani, M. *et al.* Collateral sensitivity: An evolutionary trade-off between antibiotic resistance mechanisms, attractive for dealing with drug-resistance crisis. *Health Science Reports* **6**, e1418 (2023). https://doi.org:10.1002/hsr2.1418
80 Hernando-Amado, S., Laborda, P. & Martínez, J. L. Tackling antibiotic resistance by inducing transient and robust collateral sensitivity. *Nature Communications* **14**, 1723 (2023). https://doi.org:10.1038/s41467-023-37357-4
81 Cowen, L. E. Hsp90 Orchestrates Stress Response Signaling Governing Fungal Drug Resistance. *PLOS Pathogens* **5**, e1000471 (2009). https://doi.org:10.1371/journal.ppat.1000471
82 Montañés, F. M., Pascual-Ahuir, A. & Proft, M. Repression of ergosterol biosynthesis is essential for stress resistance and is mediated by the Hog1 MAP kinase and the Mot3 and Rox1 transcription factors. *Molecular Microbiology* **79**, 1008-1023 (2011). https://doi.org:10.1111/j.1365-2958.2010.07502.x
83 Ko, Y. J. *et al.* Remodeling of global transcription patterns of *Cryptococcus neoformans* genes mediated by the stress-activated HOG signaling pathways. *Eukaryotic Cell* **8**, 1197-1217 (2009). https://doi.org:10.1128/ec.00120-09
84 Day Alison, M., McNiff Megan, M., da Silva Dantas, A., Gow Neil, A. R. & Quinn, J. Hog1 Regulates Stress Tolerance and Virulence in the Emerging Fungal Pathogen *Candida auris*. *mSphere* **3** (2018). https://doi.org:10.1128/msphere.00506-18
85 Ksiezopolska, E. *et al.* Narrow mutational signatures drive acquisition of multidrug resistance in the fungal pathogen *Candida glabrata*. *Current Biology* **31**, 5314-5326 e5310 (2021). https://doi.org:10.1016/j.cub.2021.09.084
86 Papp, C. *et al.* Triazole Evolution of *Candida parapsilosis* Results in Cross-Resistance to Other Antifungal Drugs, Influences Stress Responses, and Alters Virulence in an Antifungal Drug-Dependent Manner. *mSphere* **5** (2020). https://doi.org:10.1128/msphere.00821-20
87 Scott, N. E., Erayil, E. S., Kline, S. E. & Selmecki, A. Rapid Evolution of Multidrug Resistance in a *Candida lusitaniae* Infection during Micafungin Monotherapy. *Antimicrobial Agents and Chemotherapy* **67**, e00543-00523 (2023). https://doi.org:10.1128/aac.00543-23
88 Spettel, K. *et al.* Analysis of antifungal resistance genes in *Candida albicans* and *Candida glabrata* using next generation sequencing. *PLOS ONE* **14**, e0210397 (2019). https://doi.org:10.1371/journal.pone.0210397
89 Roemhild, R. & Andersson, D. I. Mechanisms and therapeutic potential of collateral sensitivity to antibiotics. *PLOS Pathogens* **17**, e1009172 (2021). https://doi.org:10.1371/journal.ppat.1009172
90 Cowen, L. E. *et al.* Harnessing Hsp90 function as a powerful, broadly effective therapeutic strategy for fungal infectious disease. *PNAS* **106**, 2818-2823 (2009). https://doi.org:10.1073/pnas.0813394106
91 Cowen, L. E. & Lindquist, S. Hsp90 potentiates the rapid evolution of new traits: drug resistance in diverse fungi. *Science* **309**, 2185-2189 (2005). https://doi.org:10.1126/science.1118370
92 Pachl, J. *et al.* A randomized, blinded, multicenter trial of lipid-associated amphotericin B alone versus in combination with an antibody-based inhibitor of heat shock protein 90 in patients with invasive candidiasis. *Clinical Infectious Diseases* **42**, 1404-1413 (2006). https://doi.org:10.1086/503428

93 Skrzypek, M. *et al.* The *Candida* Genome Database (CGD): incorporation of Assembly 22, systematic identifiers and visualization of high throughput sequencing data. *Nucleic Acids Research* **45**, D592–D596 (2017). https://doi.org:10.1093/nar/gkw924

94 Muñoz, J. F. *et al.* Genomic insights into multidrug-resistance, mating and virulence in *Candida auris* and related emerging species. *Nature Communications* **9**, 5346 (2018). https://doi.org:10.1038/s41467-018-07779-6

95 Munoz, J. F. *et al.* Clade-specific chromosomal rearrangements and loss of subtelomeric adhesins in *Candida auris*. *Genetics* **218** (2021). https://doi.org:10.1093/genetics/iyab029

96 Rybak, J. M. *et al.* Mutations in *TAC1B*: a Novel Genetic Determinant of Clinical Fluconazole Resistance in *Candida auris*. *mBio* **11** (2020). https://doi.org:10.1128/mBio.00365-20

97 Misas, E. *et al.* Mitochondrial Genome Sequences of the Emerging Fungal Pathogen *Candida auris*. *Frontiers in Microbiology* **11** (2020). https://doi.org:10.3389/fmicb.2020.560332

98 Rybak, J. M. *et al.* Abrogation of Triazole Resistance upon Deletion of *CDR1* in a Clinical Isolate of *Candida auris*. *Antimicrobial Agents and Chemotherapy* **63** (2019). https://doi.org:10.1128/AAC.00057-19

99 Burrack Laura, S., Todd Robert, T., Soisangwan, N., Wiederhold Nathan, P. & Selmecki, A. Genomic Diversity across *Candida auris* Clinical Isolates Shapes Rapid Development of Antifungal Resistance *In Vitro* and *In Vivo*. *mBio* **13**, e00842-00822 (2022). https://doi.org:10.1128/mbio.00842-22

100 Carolus, H. *et al.* Diagnostic allele-specific PCR for the identification of *Candida auris* clades. *Journal of Fungi* **7**, 754 (2021). https://doi.org:10.3390/jof7090754

101 CLSI. Reference Method for Broth Dilution Antifungal Susceptibility Testing of Yeasts; Approved Standard - Third Edition. CLSI document M27-A3. *Clinical and Laboratory Standards Institute* **28** (2008).

102 Boeke, J. D., LaCroute, F. & Fink, G. R. A positive selection for mutants lacking orotidine-5'-phosphate decarboxylase activity in yeast: 5-fluoro-orotic acid resistance. *Molecular Genetics and Genomics* **197**, 345-346 (1984). https://doi.org:10.1007/bf00330984

103 Foster, P. L. Methods for Determining Spontaneous Mutation Rates. *Methods in Enzymology* **409**, 195--213 , pmid = 16793403 (2006). https://doi.org:10.1016/S0076-6879(05)09012-9

104 Bellmann, R. & Smuszkiewicz, P. Pharmacokinetics of antifungal drugs: practical implications for optimized treatment of patients. *Infection* **45**, 737-779 (2017). https://doi.org:10.1007/s15010-017-1042-z

105 Caballero, U. *et al. In Vitro* Pharmacokinetic/Pharmacodynamic Modelling and Simulation of Amphotericin B against *Candida auris*. *Pharmaceutics* **13** (2021). https://doi.org:10.3390/pharmaceutics13111767

106 Caballero, U. *et al.* PK/PD modeling and simulation of the *in vitro* activity of the combinations of isavuconazole with echinocandins against *Candida auris*. *CPT: Pharmacometrics & Systems Pharmacology* **12**, 770-782 (2023). https://doi.org:10.1002/psp4.12949

107 Hünniger, K. *et al.* A Virtual Infection Model Quantifies Innate Effector Mechanisms and *Candida albicans* Immune Escape in Human Blood. *PLOS Computational Biology* **10**, e1003479 (2014). https://doi.org:10.1371/journal.pcbi.1003479

108 Praußе, M. T. *et al.* Predictive virtual infection modeling of fungal immune evasion in human whole blood. *Frontiers in Immunology* **9**, 560 (2018). https://doi.org:10.3389/fimmu.2018.00560

109 Ankomah, P. & Levin, B. R. Exploring the collaboration between antibiotics and the immune response in the treatment of acute, self-limiting infections. *PNAS* **111**, 8331-8338 (2014). https://doi.org:10.1073/pnas.1400352111

110 Kochin, B. F., Yates, A. J., de Roode, J. C. & Antia, R. On the Control of Acute Rodent Malaria Infections by Innate Immunity. *PLOS ONE* **5**, e10444 (2010). https://doi.org:10.1371/journal.pone.0010444

111 Reuß , O., Vik, A., Kolter, R. & Morschhauser, J. The SAT1 flipper, an optimized tool for gene disruption in *Candida albicans*. *Gene* **341**, 119-127 (2004). https://doi.org:10.1016/j.gene.2004.06.021

112 Schikora-Tamarit, M. A. & Gabaldon, T. PerSVade: personalized structural variant detection in any species of interest. *Genome Biology* **23**, 175 (2022). https://doi.org:10.1186/s13059-022-02737-4

113 Andrews, S. *FastQC: A Quality Control Tool for High Throughput Sequence Data*, <http://www.bioinformatics.babraham.ac.uk/projects/fastqc/> (2010).

114 Bolger, A. M., Lohse, M. & Usadel, B. Trimmomatic: a flexible trimmer for Illumina sequence data. *Bioinformatics* **30**, 2114-2120 (2014). https://doi.org:10.1093/bioinformatics/btu170

115 Danecek, P. *et al.* Twelve years of SAMtools and BCFtools. *Gigascience* **10** (2021). https://doi.org:10.1093/gigascience/giab008

116 Poplin, R. *et al.* Scaling accurate genetic variant discovery to tens of thousands of samples *bioRxiv (preprint)* (2018). https://doi.org:10.1101/201178

117 Garisson, E. & Marth, G. Haplotype-based variant detection from short-read sequencing (preprint). *arXiv (preprint)* (2012). https://doi.org:10.48550/arXiv.1207.3907

118 McLaren, W. *et al.* The Ensembl Variant Effect Predictor. *Genome Biology* **17**, 122 (2016). https://doi.org:10.1186/s13059-016-0974-4

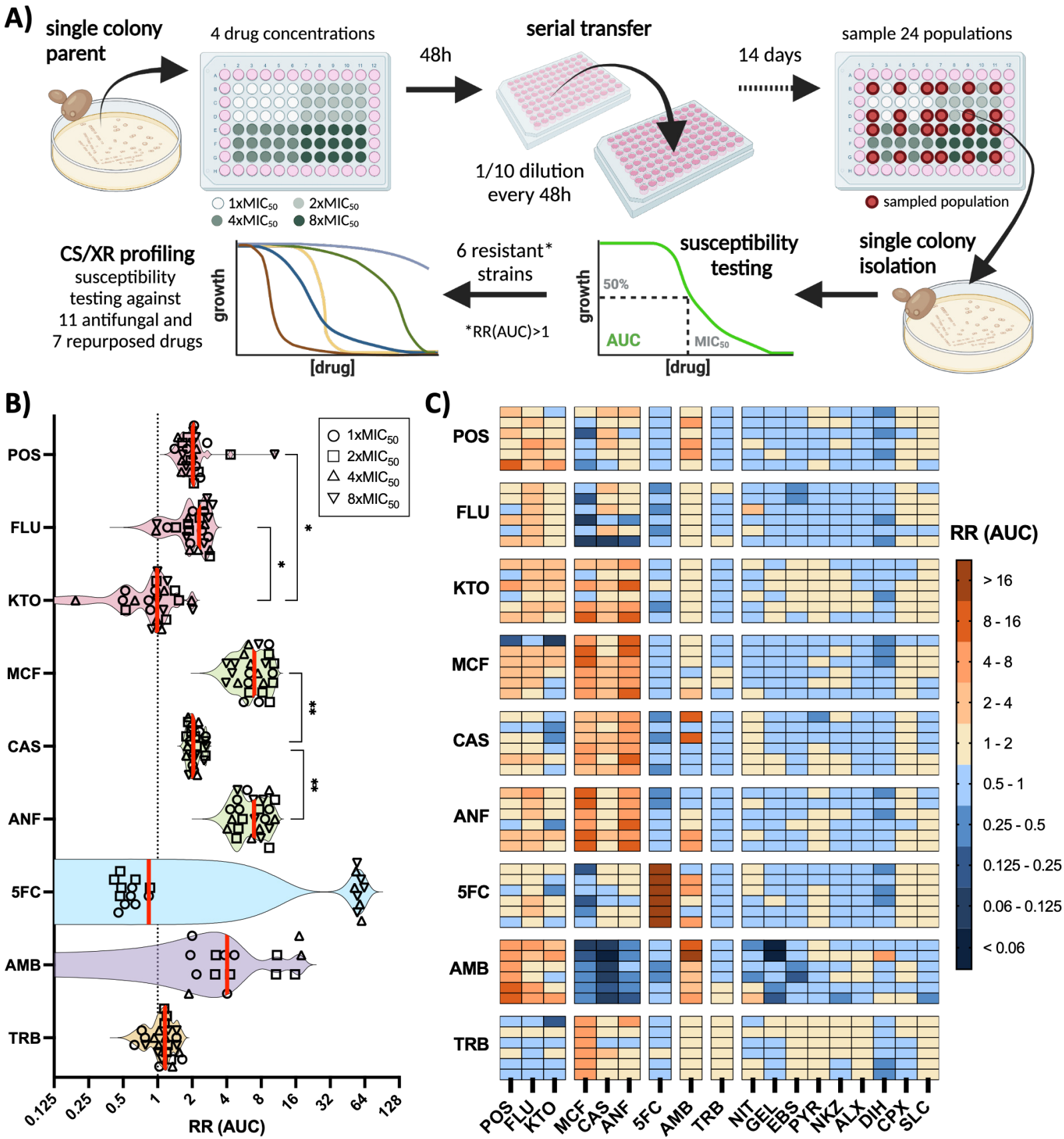
A)
single colony parent
4 drug concentrations
1xMIC50
2xMIC50
4xMIC50
8xMIC50
48h
serial transfer
1/10 dilution every 48h
14 days
sample 24 populations
sampled population
single colony isolation
susceptibility testing
growth
50%
AUC
MIC50
[drug]
6 resistant* strains
*RR(AUC)>1
CS/XR profiling
susceptibility testing against 11 antifungal and 7 repurposed drugs
B)
POS
FLU
KTO
MCF
CAS
ANF
5FC
AMB
TRB
0.125
0.25
0.5
1
2
4
8
16
32
64
128
RR (AUC)
C)
RR (AUC)
> 16
8 - 16
4 - 8
2 - 4
1 - 2
0.5 - 1
0.25 - 0.5
0.125 - 0.25
0.06 - 0.125
< 0.06
NIT
GEL
EBS
PYR
NKZ
ALX
DIH
CPX
SLC

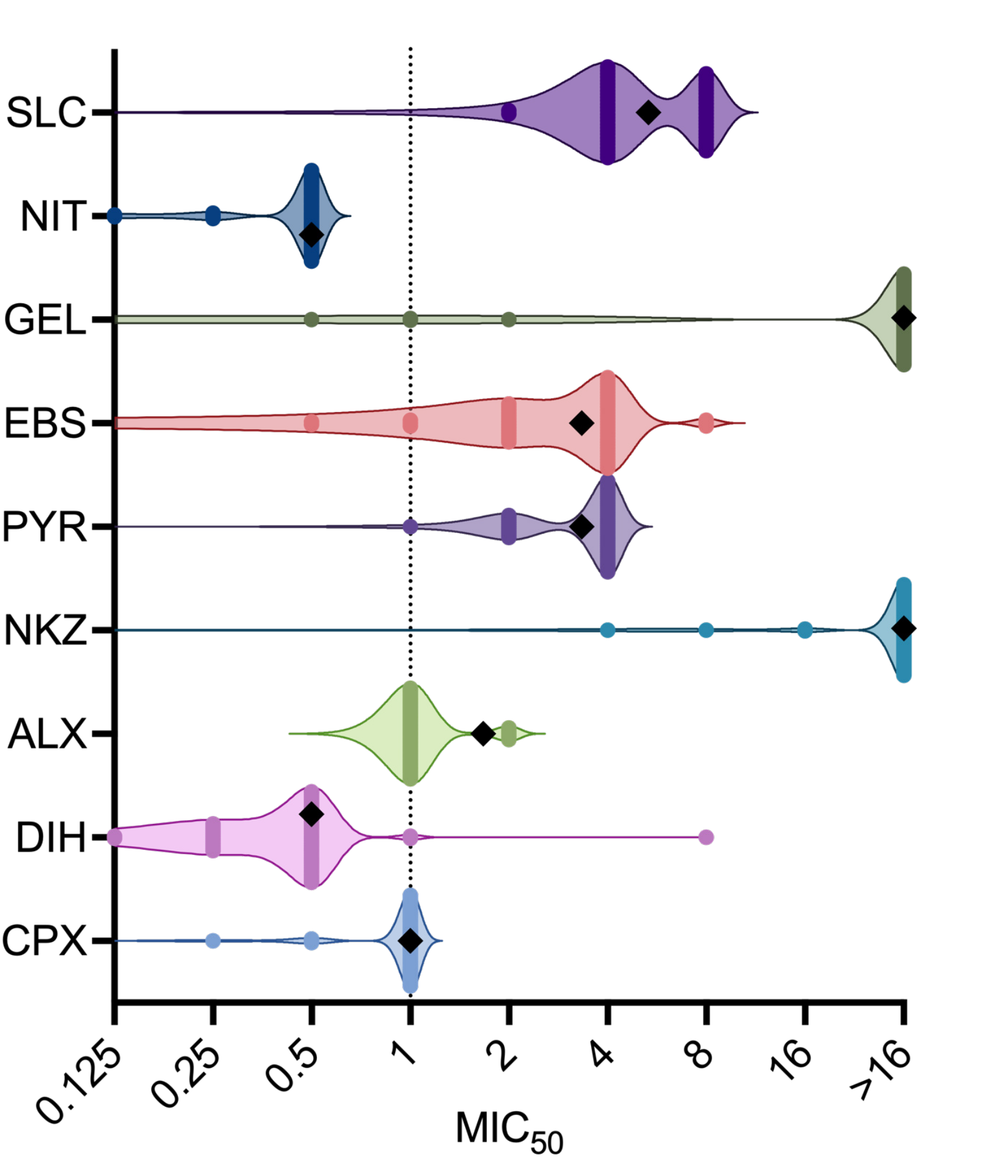
SLC
NIT
GEL
EBS
PYR
NKZ
ALX
DIH
CPX
0.125
0.25
0.5
1
2
4
8
16
>16
MIC50

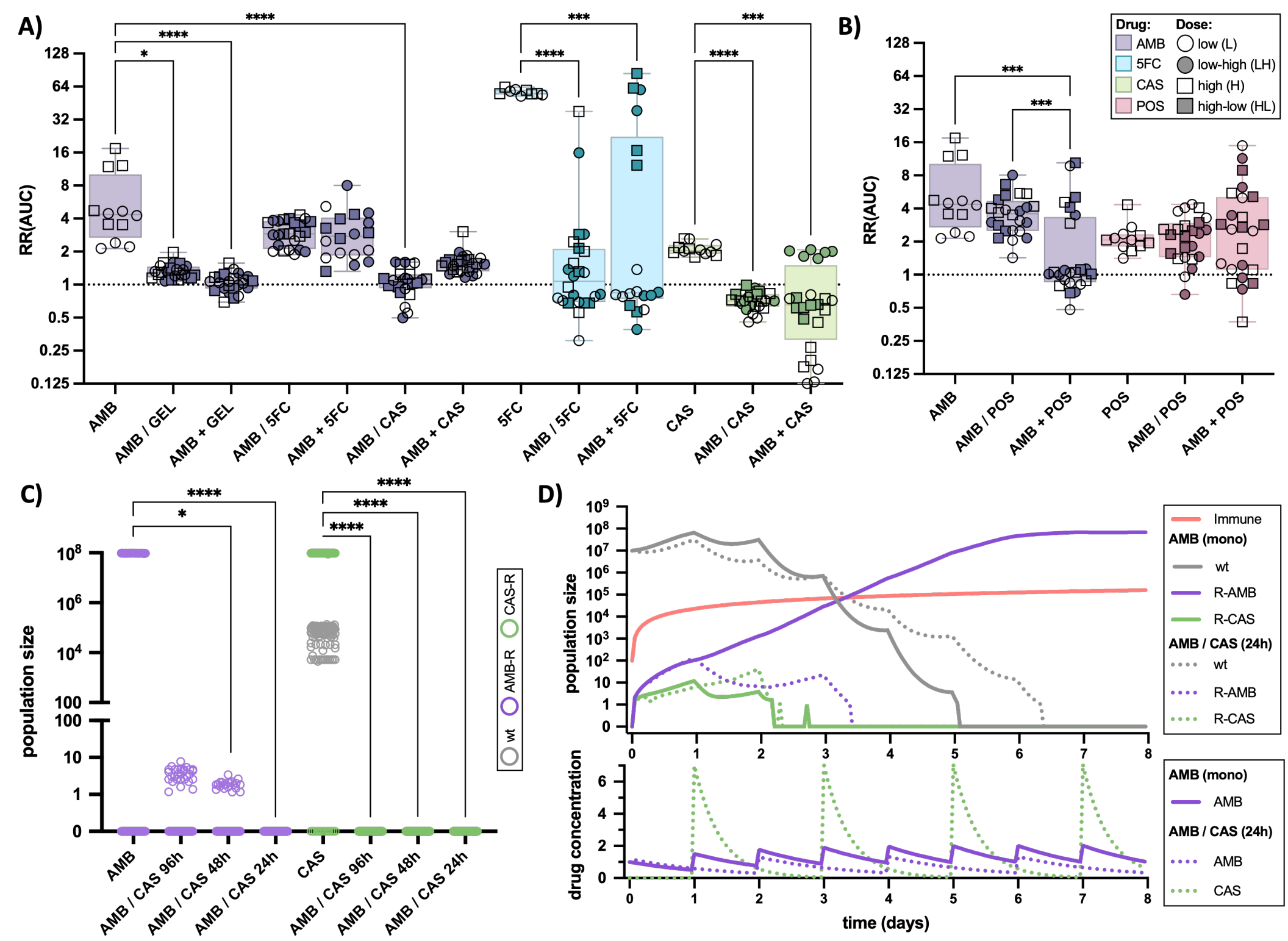
A)
RR(AUC)
128
64
32
16
8
4
2
1
0.5
0.25
0.125
****
****
*
***
****
***
****
AMB
AMB / GEL
AMB + GEL
AMB / 5FC
AMB + 5FC
AMB / CAS
AMB + CAS
5FC
AMB / 5FC
AMB + 5FC
CAS
AMB / CAS
AMB + CAS
B)
Drug:
AMB
5FC
CAS
POS
Dose:
low (L)
low-high (LH)
high (H)
high-low (HL)
RR(AUC)
128
64
32
16
8
4
2
1
0.5
0.25
0.125
***
***
AMB
AMB / POS
AMB + POS
POS
AMB / POS
AMB + POS
C)
population size
10^8
10^6
10^4
100
100
10
1
0
****
*
****
****
****
AMB
AMB / CAS 96h
AMB / CAS 48h
AMB / CAS 24h
CAS
AMB / CAS 96h
AMB / CAS 48h
AMB / CAS 24h
CAS-R
AMB-R
wt
D)
population size
10^9
10^8
10^7
10^6
10^5
10^4
10^3
10^2
10
1
0
0
1
2
3
4
5
6
7
8
Immune
AMB (mono)
wt
R-AMB
R-CAS
AMB / CAS (24h)
wt
R-AMB
R-CAS
drug concentration
6
4
2
0
0
1
2
3
4
5
6
7
8
time (days)
AMB (mono)
AMB
AMB / CAS (24h)
AMB
CAS

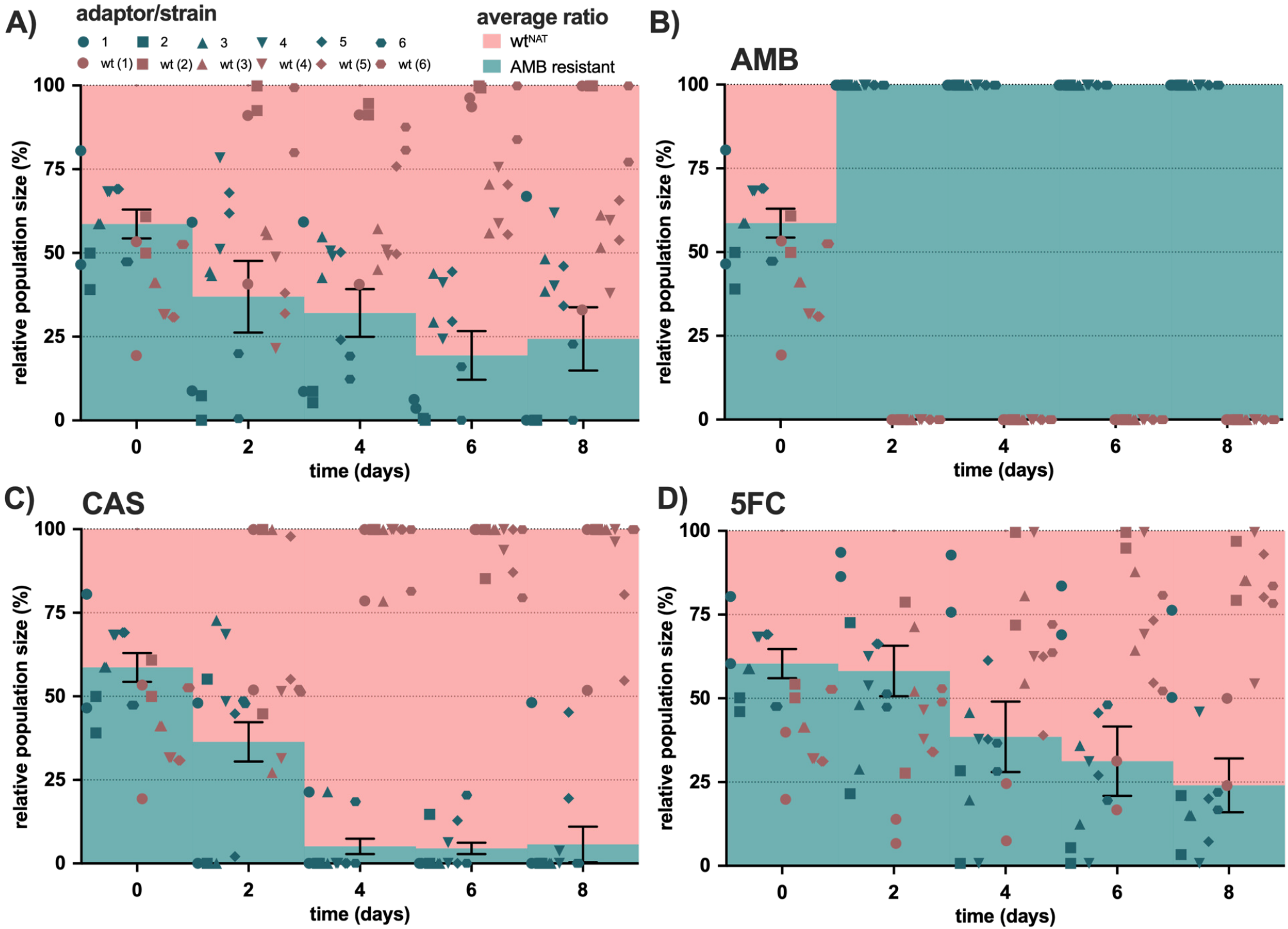
A)
adaptor/strain
1
2
3
4
5
6
wt (1)
wt (2)
wt (3)
wt (4)
wt (5)
wt (6)
average ratio
wtNAT
AMB resistant
relative population size (%)
time (days)
B)
AMB
C)
CAS
D)
5FC

clade	strain	variant *ERG* gene	variant	AMB	POS	FLU	MCF	CAS	ANF	5FC	GEL
I	1	*ERG11*	M504I	12.30	5.77	4.88	0.10	0.07	0.40	0.51	0.05
I	2	*ERG11(+ERG3)*	E165* (T308M)	19.70	7.40	3.98	0.24	0.05	0.41	0.60	0.03
I	3	*ERG6*	R318I	2.22	4.39	1.68	0.34	0.11	0.59	0.34	0.95
I	4	*ERG6*	Y177*	2.35	4.87	1.04	0.32	0.11	0.42	0.27	0.81
I	5	*NCP1*	Q587*	2.49	9.07	4.30	0.28	0.14	0.33	0.52	0.33
I	6	*NCP1*	T451fs	4.45	10.00	4.18	0.29	0.11	0.20	0.63	0.17
III	7	*ERG11(+ERG3)*	T369M (G108*)	4.90	3.72	1.42	0.11	0.13	0.31	8.49	0.23
III	8	*ERG11*	M306I	8.40	3.45	0.93	0.15	0.18	0.43	2.21	0.14
III	9	*NCP1*	Transl.	2.47	3.09	0.95	0.11	0.18	0.36	2.68	0.43
III	10	*ERG6*	K234_D236del	2.94	1.47	0.95	0.13	0.21	0.27	1.89	0.77
III	11	*NCP1*	Q368*	3.90	4.52	0.76	0.14	0.26	0.22	2.46	0.68
III	12	*ERG6*	E86fs	4.61	0.71	1.26	0.10	0.23	0.32	0.93	0.71
IV	13	*ERG6*	F311fs	2.74	1.85	1.22	0.74	0.09	1.32	0.91	0.57
IV	14	*ERG6*	E329*	2.43	0.55	0.53	0.84	0.09	0.93	1.37	0.40
IV	15	*ERG6*	R100fs	2.09	1.29	0.73	0.67	0.04	1.25	1.19	0.53
IV	16	*ERG12*	E18Q	1.91	0.11	0.13	2.09	0.12	1.33	1.13	0.80
IV	17	*HMG1*	R983S	1.48	0.10	0.13	0.97	0.58	0.78	1.43	0.58
IV	18	*ERG10*	T244N	1.41	0.13	0.22	1.78	0.30	0.46	1.60	0.67
II	19	*ERG11(+ERG3)*	E429* (W182*)	2.51	10.50	8.39	0.49	0.78	0.92	2.60	0.07

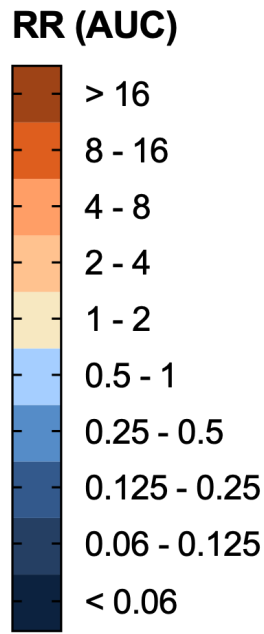

type	drug	abbreviation	MIC_{50}
antifungal	*posaconazole*	*POS*	0.25
	fluconazole	*FLU*	1
	ketoconazole	*KTO*	0.167
	micafungin	*MCF*	1
	caspofungin	*CAS*	1
	anidulafungin	*ANF*	1
	flucytosine (5-fluorocytosine)	*5FC*	0.125
	amphotericin B	*AMB*	1
	terbinafine	*TRB*	2.833
	nikkomycin Z	NKZ	>16
	ciclopirox ethanolamine	CPX	1
antibacterial	nitroxoline	NIT	0.5
	alexidine dihydrochloride	ALX	1.667
anticancer	geldanamycin	GEL	>16
anti-inflammatory	ebselen	EBS	3.333
antiplatelet	suloctidil	SLC	5.333
antiparasitic	pyrvinium pamoate	PYR	3.333
	diiodohydroxyquinoline	DIH	0.5

AUC	effect (MFC)
110.5	Fungicidal (16)
292.2	Fungistatic
236.9	Fungistatic
149.8	Fungicidal (4)
658.2	Fungistatic
124.1	Fungicidal (4)
25.9	Fungicidal (0.5)
61.5	Fungicidal (2)
695.7	Fungistatic
1631	Fungistatic
76.1	Fungicidal (2)
46.9	Fungicidal (2)
116.1	Fungicidal (8)
1675	Fungistatic
359.1	Fungicidal (8)
429.7	Fungicidal (16)
296	Fungicidal (16)
105.6	Fungicidal (1)

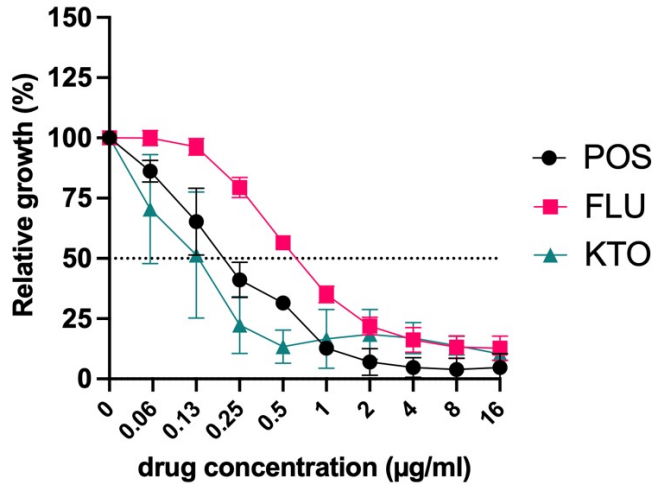
Relative growth (%)
150
125
100
75
50
25
0
0
0.06
0.13
0.25
0.5
1
2
4
8
16
drug concentration (µg/ml)
POS
FLU
KTO

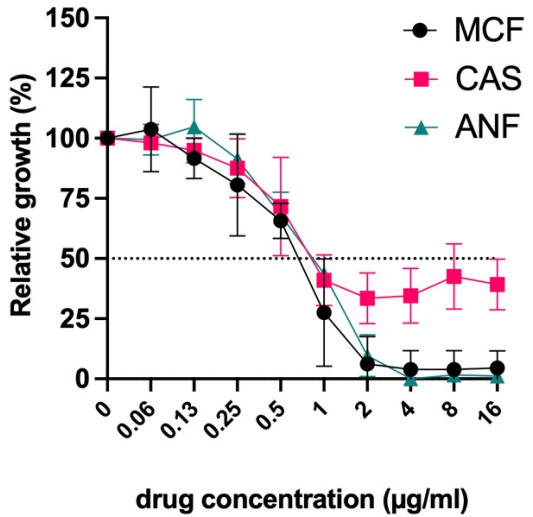
Relative growth (%)
drug concentration (µg/ml)
MCF
CAS
ANF

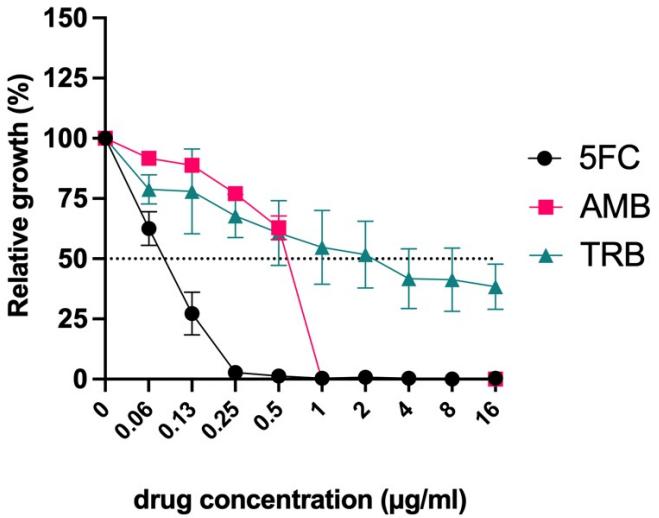
Relative growth (%)
drug concentration (µg/ml)
5FC
AMB
TRB

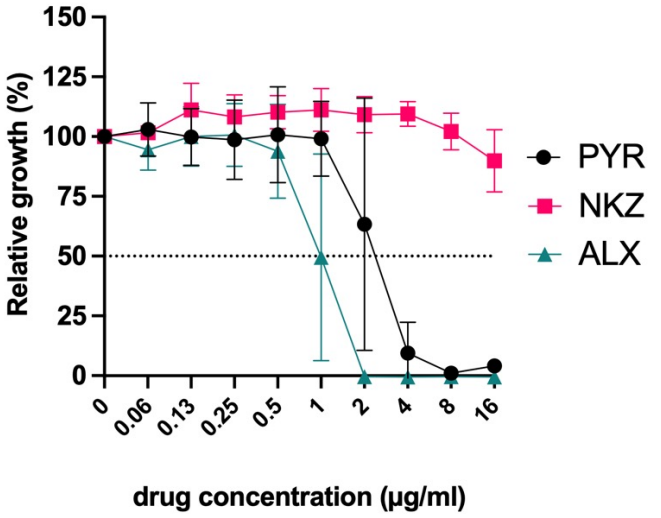
Relative growth (%)
drug concentration (µg/ml)
PYR
NKZ
ALX

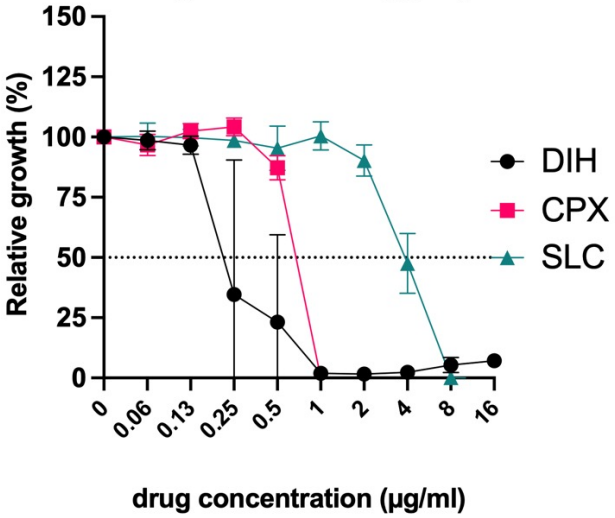
Relative growth (%)
drug concentration (µg/ml)
DIH
CPX
SLC

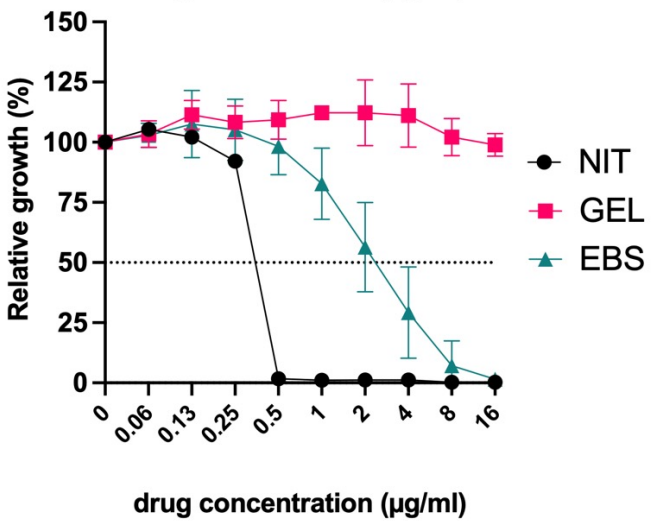
Relative growth (%)
drug concentration (µg/ml)
NIT
GEL
EBS

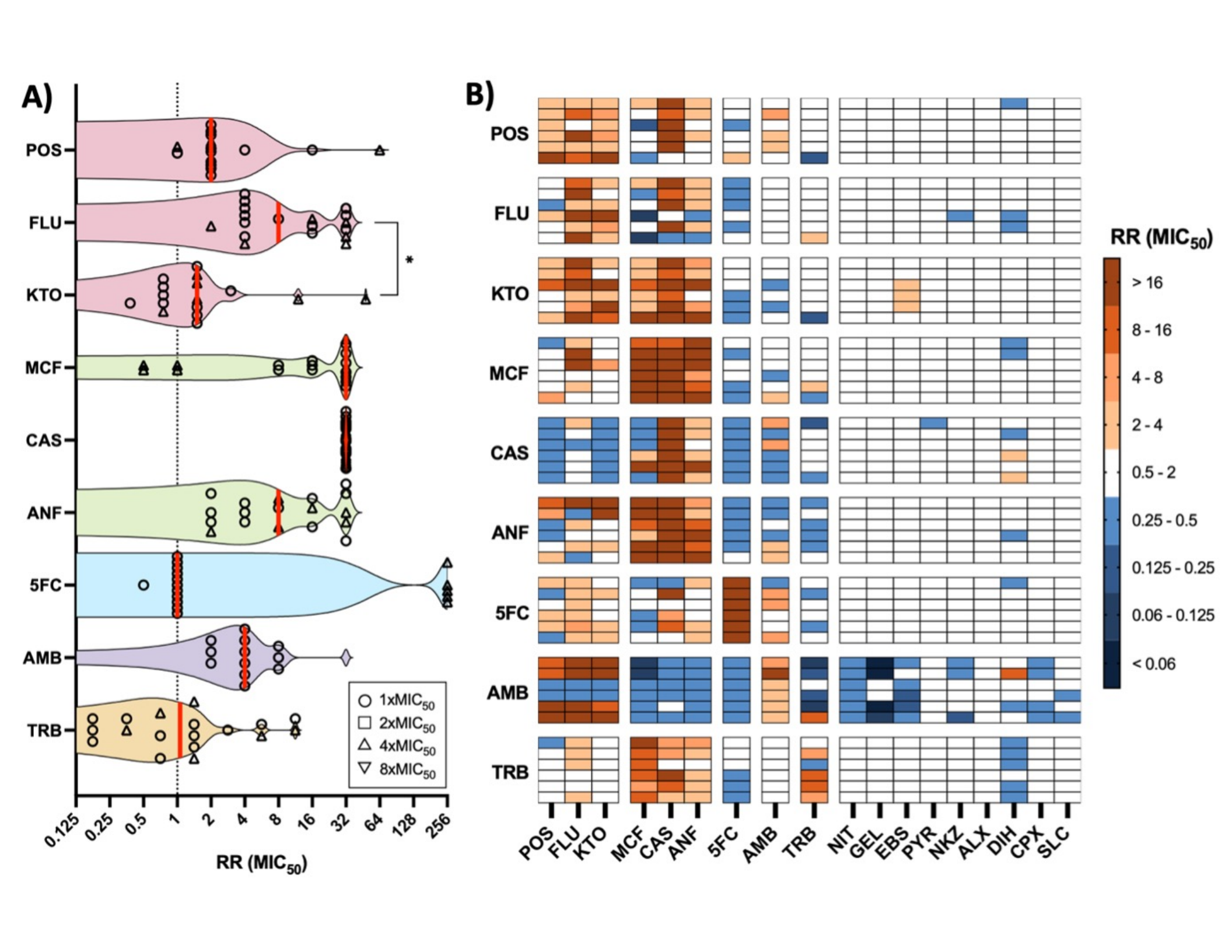
A)
POS
FLU
KTO
MCF
CAS
ANF
5FC
AMB
TRB
*
1xMIC50
2xMIC50
4xMIC50
8xMIC50
0.125
0.25
0.5
1
2
4
8
16
32
64
128
256
RR (MIC50)
B)
POS
FLU
KTO
MCF
CAS
ANF
5FC
AMB
TRB
NIT
GEL
EBS
PYR
NKZ
ALX
DIH
CPX
SLC
RR (MIC50)
> 16
8 - 16
4 - 8
2 - 4
0.5 - 2
0.25 - 0.5
0.125 - 0.25
0.06 - 0.125
< 0.06

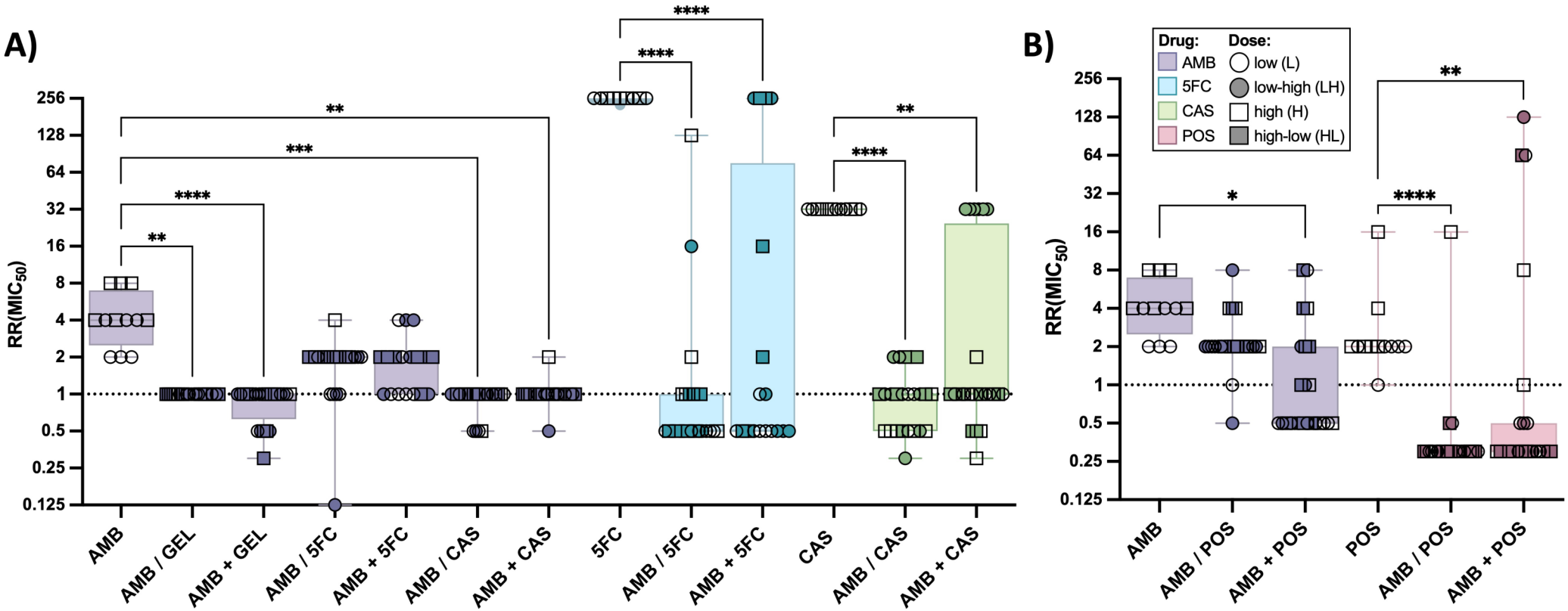
A)
B)
RR(MIC50)
256
128
64
32
16
8
4
2
1
0.5
0.25
0.125
**
***
****
*
AMB
AMB / GEL
AMB + GEL
AMB / 5FC
AMB + 5FC
AMB / CAS
AMB + CAS
5FC
AMB / 5FC
AMB + 5FC
CAS
AMB / CAS
AMB + CAS
AMB / POS
AMB + POS
POS
Drug:
AMB
5FC
CAS
POS
Dose:
low (L)
low-high (LH)
high (H)
high-low (HL)

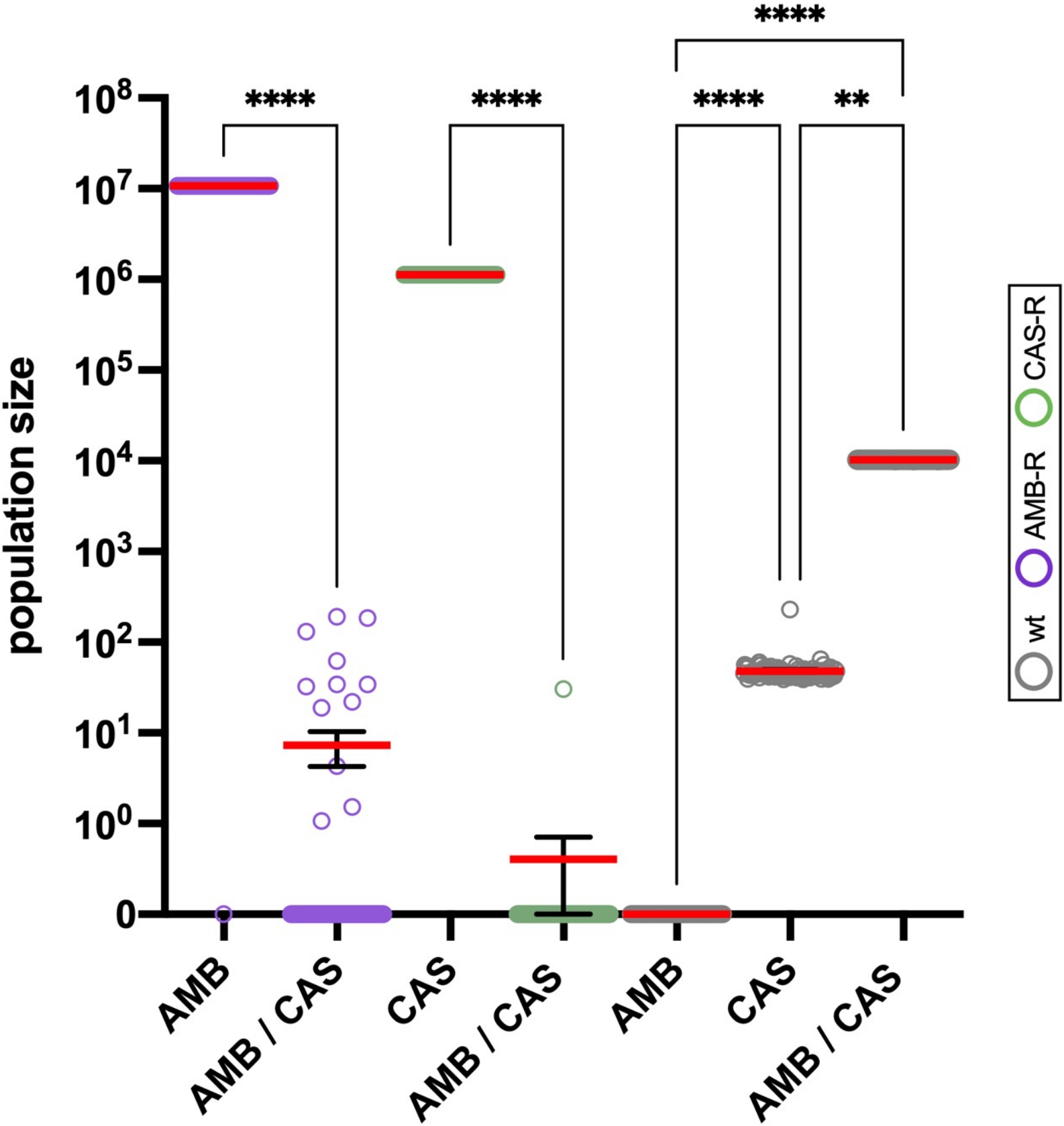
****
****
****
****
**
population size
10^8
10^7
10^6
10^5
10^4
10^3
10^2
10^1
10^0
0
AMB
AMB / CAS
CAS
AMB / CAS
AMB
CAS
AMB / CAS
wt
AMB-R
CAS-R

```
CaNEUTL   97  AGAAAAAGCAATCACAGCTTATTAACGAT-TC---GTGTTTAAATAATCAATTGAAAGGA
CauNEUTL  56  AGAGAACCCTGTGACTGCTTTT---CGCTATCAGGGGGTTGA----------TGGAGGGG

CaNEUTL   153 AAATAGAAGATTTTTGAAAAAAAGTTATTGGTATTTATTAACTTAATATATCAGTAACAT
CauNEUTL  103 CACCCGAAGTTATGTGCA----------GGGAGCTTTTCAC-TAGTTTTT------GAT

CaNEUTL   213 CAAGAGAAAGAAACTGA-ATTATAAACAGAGT----------------------ATG
CauNEUTL  145 AAACAGAAGGGCTCTGAGAGGGT---CAGCGTTGCGGGTGCCCGACGTTGGCTAGAAATG

CaNEUTL   247 TGAAGCAA--------TTGCAATT-GCAATTATTAGAGATCCAGAAAACTGAATTGTGCT
CauNEUTL  202 TTAAACAAAAATCGAGTTG--ATTGGCTGTTGGGAGA-ATGCAACAAGCTGTATAGT-CT

CaNEUTL   297 ----------TGAATACCACTTGTTTAGGAAGGACGATGAAGGAGAGAAAGTAGTAAGAC
CauNEUTL  258 GGATGAGGTGTGCAT--CACGT------GACGCGTGTTGATGGA-AAAAAGTGCGATCAC

CaNEUTL   348 A--ATATGACTTTGGACAGATATGAGATAAAAG--TTTTA------AAGGACAAGAAAAG
CauNEUTL  309 AGGATAAG-CCTTGCATAGAAAGGA-AAAAAAGCATTTGAGCAGAGAGGGAAAAAAAAA-

CaNEUTL   398 GTTCGGGTTA-AAAGATGAGTA-TTGTATTTTTTCAAAATAT------CAA---------
CauNEUTL  365 --------TATATATATCTCTACTTG-ATCTCATCAATTTATCCTTCACAAAACCCGCCG

CaNEUTL   440 ------TGCTT-----TTTCTGTTCTTGGGTTAGTGGTACCACCATTGGTGATA------
CauNEUTL  417 CTAGGCTACTTCCCCGTTTATTTTCTTTCTTTGCTGCT-----CTTCGTTGAGACAGAAG

CaNEUTL   483 -AAA---------CCTTTGGGGAGCCTCCTCCGAGCTTTCTCTTTGTTACTTTTTTTCTC
CauNEUTL  472 GAAAACAAATATCCATTTGAAAAGACT---------TTT---TTT-----TTTTATTCAC

CaNEUTL   534 AACTGATACTTGTCATT
CauNEUTL  515 GAATTTTTCCTGTCTTT
```

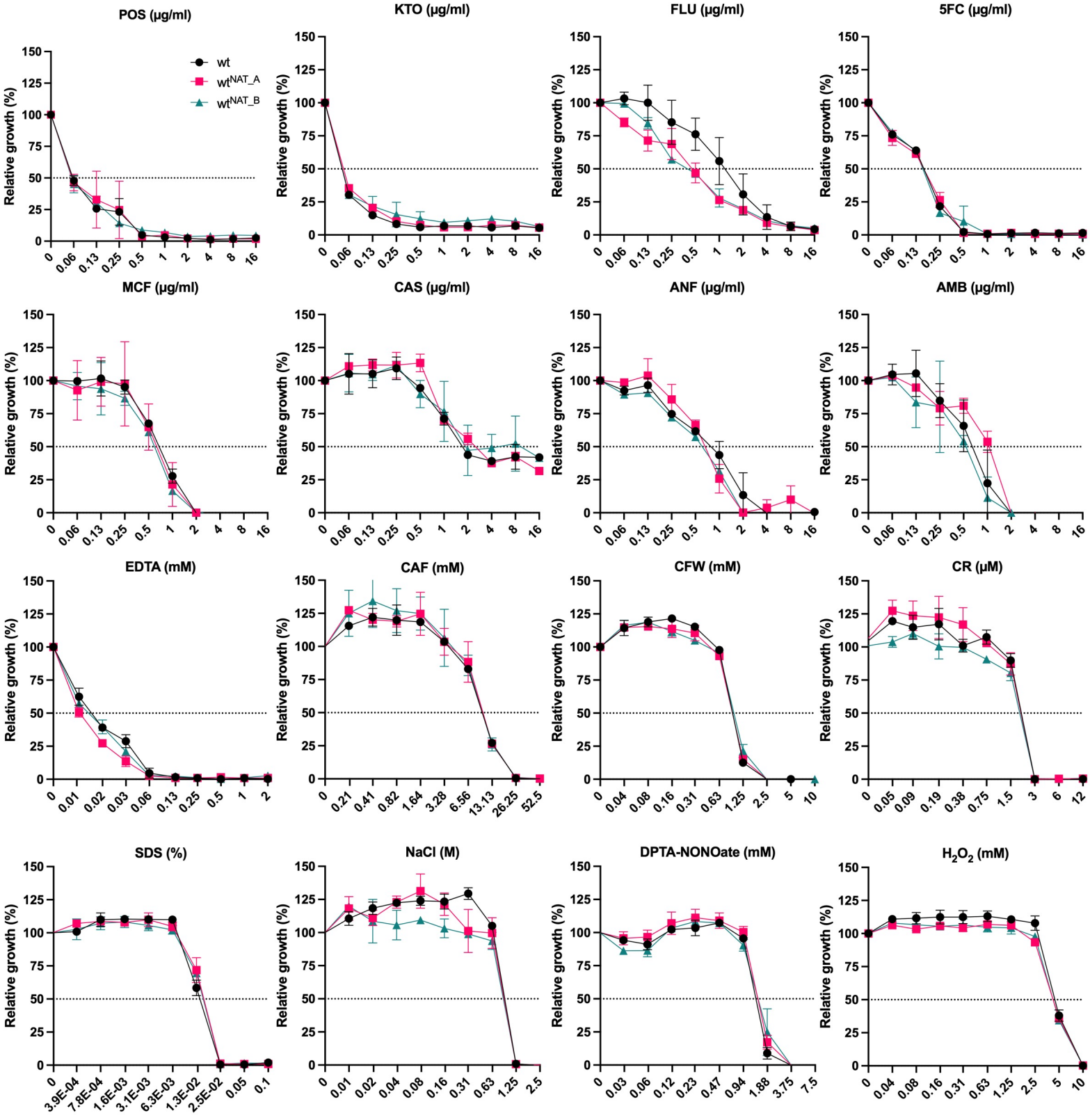
POS (µg/ml)
KTO (µg/ml)
FLU (µg/ml)
5FC (µg/ml)
MCF (µg/ml)
CAS (µg/ml)
ANF (µg/ml)
AMB (µg/ml)
EDTA (mM)
CAF (mM)
CFW (mM)
CR (µM)
SDS (%)
NaCl (M)
DPTA-NONOate (mM)
H2O2 (mM)
Relative growth (%)
wt
wtNAT_A
wtNAT_B

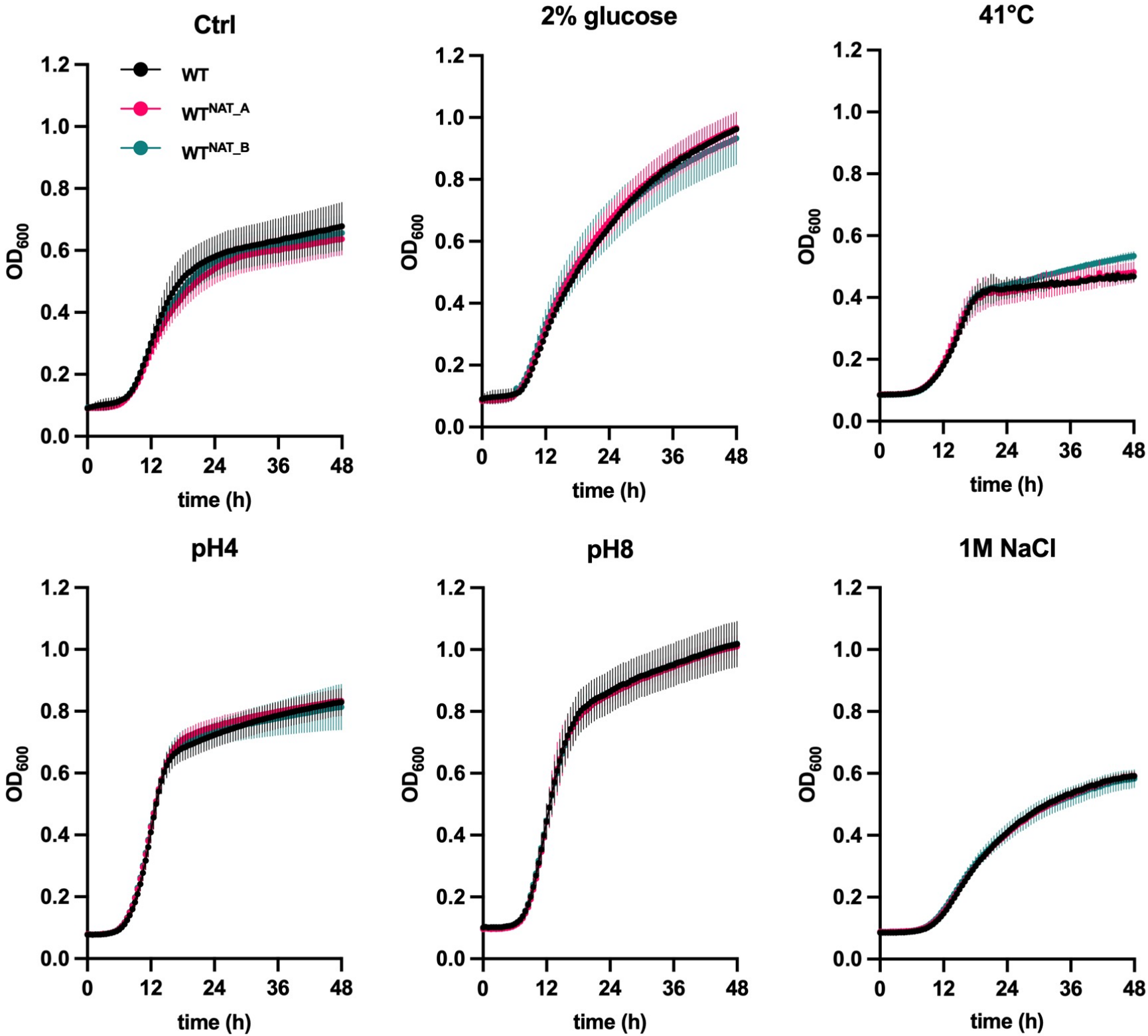
Ctrl
2% glucose
41°C
pH4
pH8
1M NaCl
WT
WT^NAT_A
WT^NAT_B
OD600
time (h)
0.0
0.2
0.4
0.6
0.8
1.0
1.2
0
12
24
36
48

clade	strain	variant *ERG* gene	variant	AMB	POS	FLU	MCF	CAS	ANF	5FC	GEL
I	1	*ERG11*	M504I	8.00	16.00	32.00	0.06	0.50	0.50	0.50	0.03
I	2	*ERG11(+ERG3)*	E165* (T308M)	32.00	16.00	32.00	0.06	0.25	0.50	0.50	0.02
I	3	*ERG6*	R318I	2.00	0.25	0.25	0.50	0.50	0.50	0.50	1.00
I	4	*ERG6*	Y177*	2.00	0.25	0.25	0.50	0.50	0.50	0.50	1.00
I	5	*NCP1*	Q587*	2.00	128.00	32.00	0.50	1.00	0.50	0.50	0.03
I	6	*NCP1*	T451fs	4.00	128.00	32.00	0.25	0.50	0.25	0.50	0.06
III	7	*ERG11(+ERG3)*	T369M (G108*)	4.00	256.00	1.00	0.50	1.00	0.50	8.00	0.13
III	8	*ERG11*	M306I	8.00	256.00	1.00	1.00	1.00	1.00	2.00	0.06
III	9	*NCP1*	Transl.	2.00	256.00	1.00	1.00	2.00	1.00	4.00	0.25
III	10	*ERG6*	K234_D236del	4.00	16.00	1.00	2.00	1.00	2.00	2.00	0.50
III	11	*NCP1*	Q368*	2.00	256.00	1.00	2.00	2.00	1.00	2.00	0.50
III	12	*ERG6*	E86fs	4.00	0.50	1.00	1.00	2.00	2.00	0.50	1.00
IV	13	*ERG6*	F311fs	2.00	32.00	1.00	2.00	1.00	2.00	0.50	0.50
IV	14	*ERG6*	E329*	2.00	1.00	0.25	1.00	1.00	2.00	0.50	0.25
IV	15	*ERG6*	R100fs	2.00	1.00	0.25	0.50	1.00	2.00	0.50	0.50
IV	16	*ERG12*	E18Q	2.00	1.00	0.13	2.00	4.00	2.00	0.50	1.00
IV	17	*HMG1*	R983S	2.00	1.00	0.50	1.00	1.00	1.00	1.00	0.50
IV	18	*ERG10*	T244N	2.00	1.00	0.50	2.00	2.00	1.00	1.00	0.50
II	19	*ERG11(+ERG3)*	E429* (W182*)	2.00	16.00	16.00	1.00	1.00	0.50	1.00	0.03

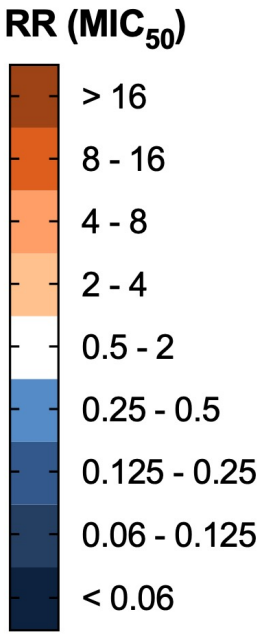

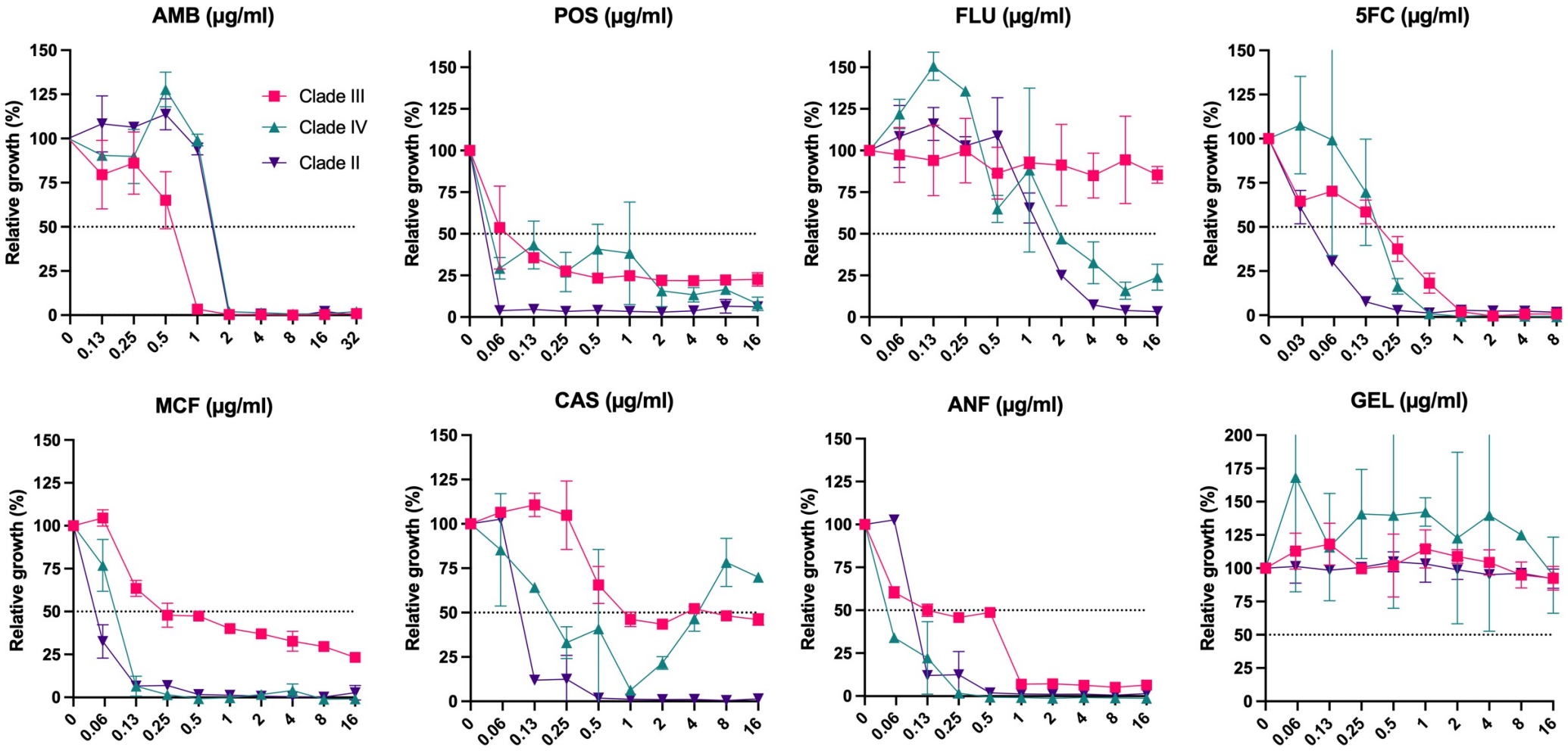
AMB (µg/ml)
POS (µg/ml)
FLU (µg/ml)
5FC (µg/ml)
MCF (µg/ml)
CAS (µg/ml)
ANF (µg/ml)
GEL (µg/ml)
Relative growth (%)
Clade III
Clade IV
Clade II

A)

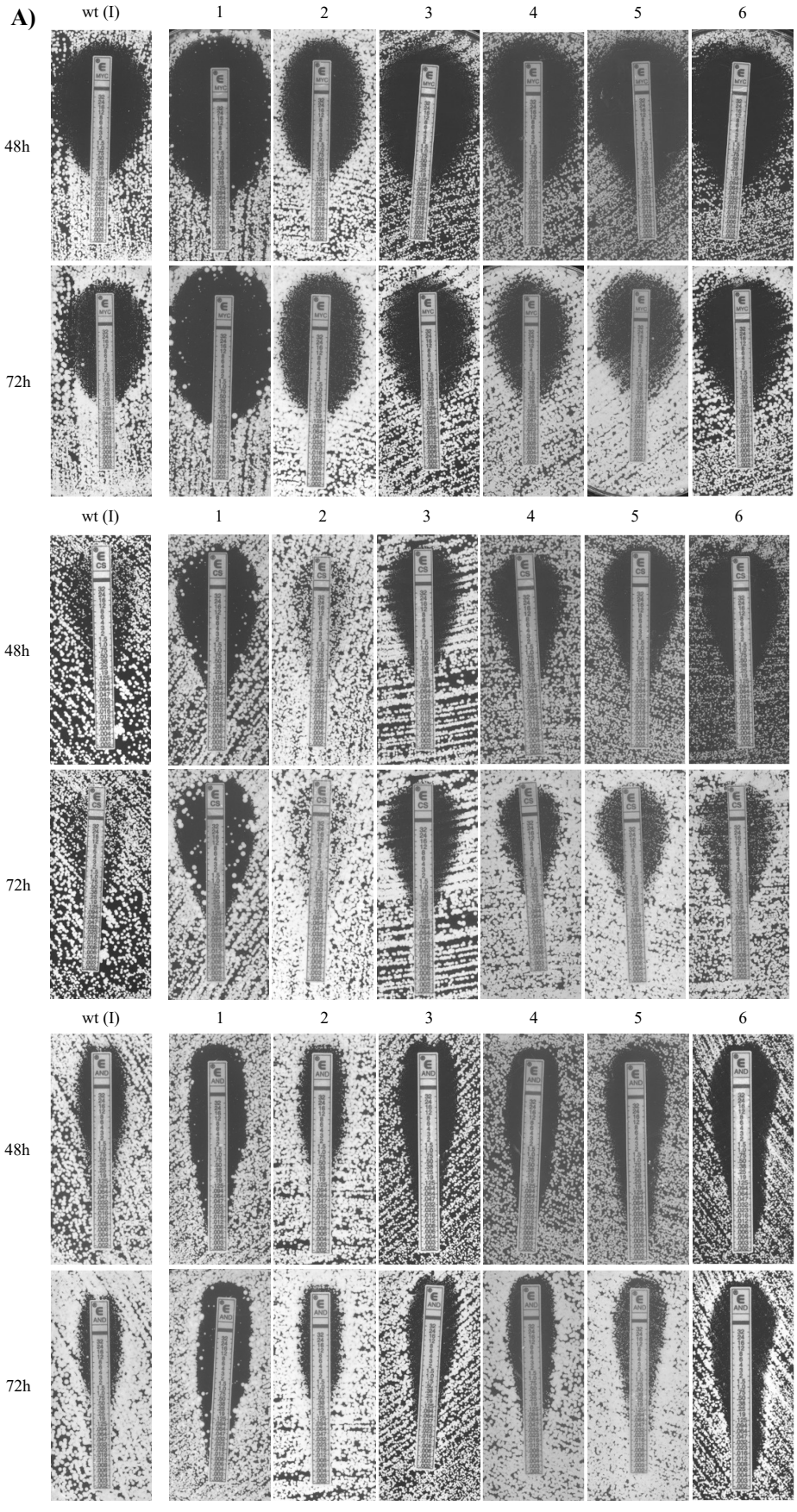

strain	MIC
wt	0.125
1	0.047
2	0.19
3	0.094
4	0.125
5	0.064
6	0.064

strain	MIC
wt	0.75
1	0.064
2	0.38
3	0.25
4	0.25
5	0.19
6	0.19

strain	MIC
wt	0.064
1	0.012
2	0.094
3	0.064
4	0.047
5	0.047
6	0.032

B)

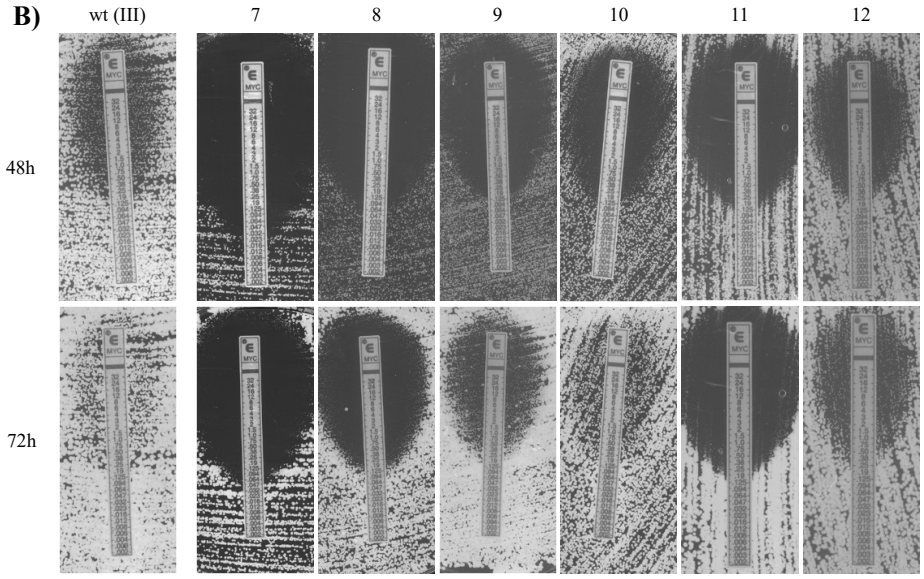

strain	MIC
wt	0.19
7	0.023
8	0.125
9	0.125
10	0.125
11	0.125
12	0.25

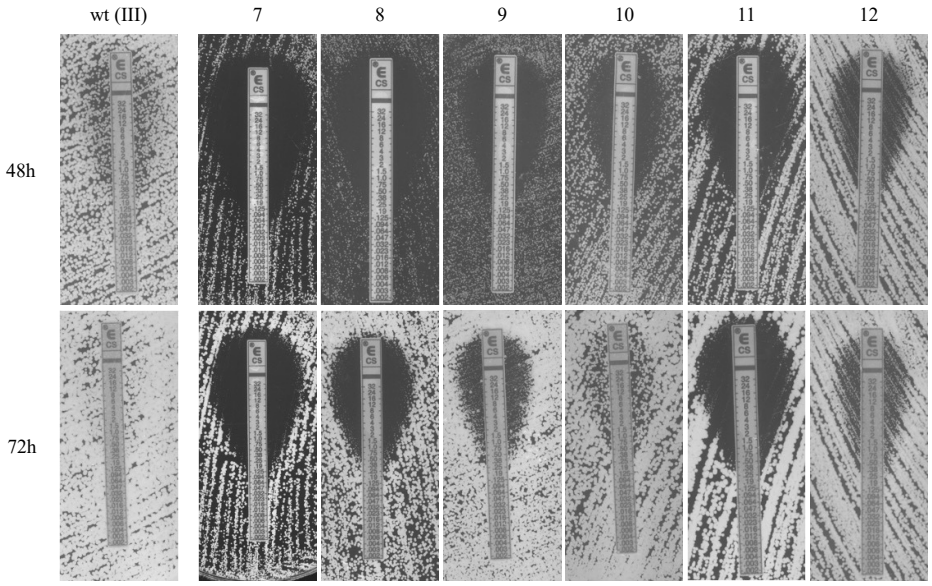

strain	MIC
wt	0.5
7	0.03
8	0.25
9	0.25
10	0.5
11	0.25
12	0.38

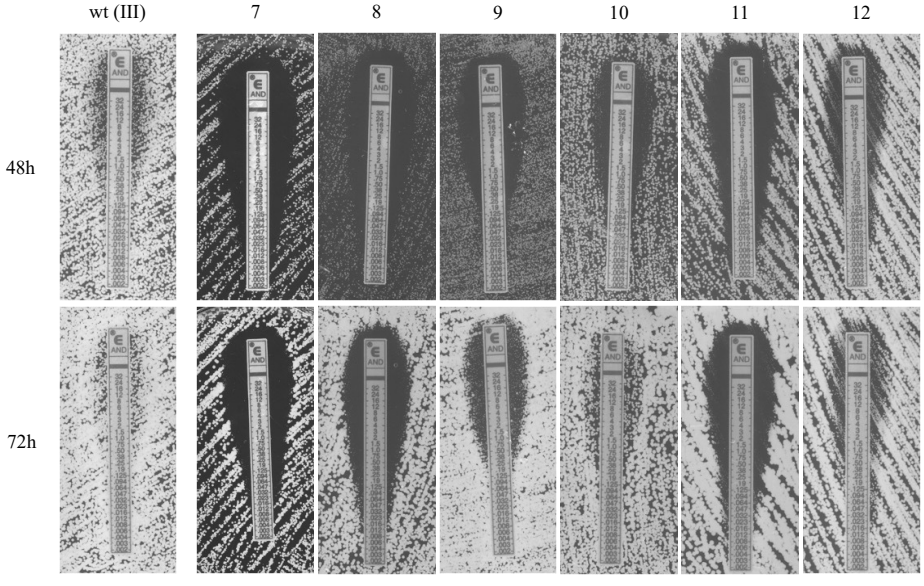

strain	MIC
wt	0.25
7	0.012
8	0.016
9	0.19
10	0.094
11	0.008
12	0.094

C)

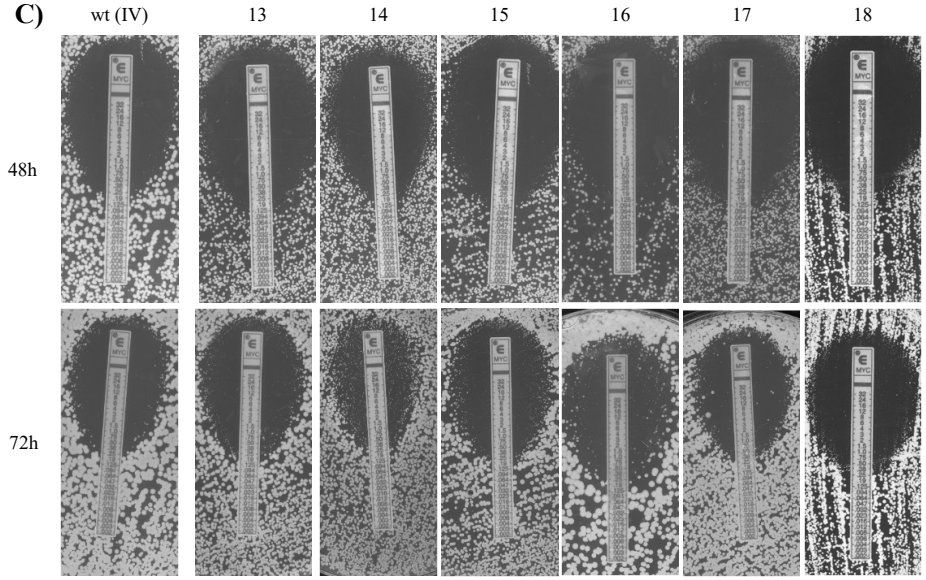

strain	MIC
wt	0.19
13	0.125
14	0.19
15	0.125
16	0.125
17	0.125
18	0.25

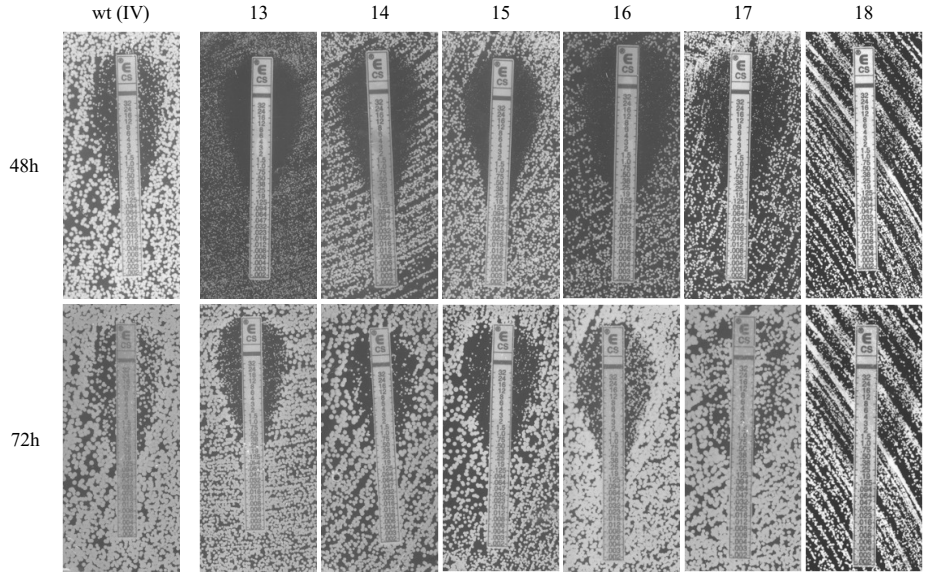

strain	MIC
wt	0.19
13	0.25
14	0.25
15	0.19
16	0.25
17	0.25
18	0.38

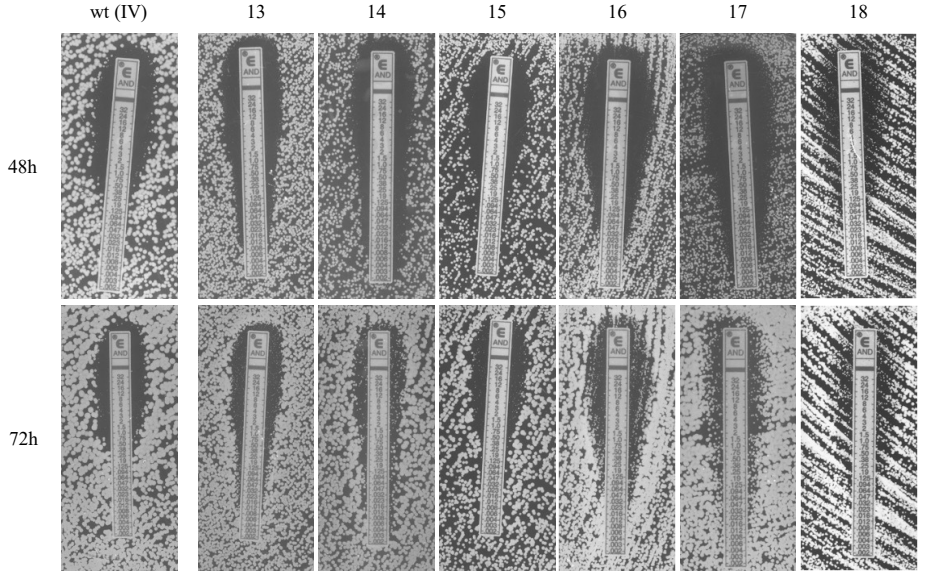

strain	MIC
wt	0.38
13	0.016
14	0.006
15	0.38
16	0.047
17	0.008
18	0.064

D)

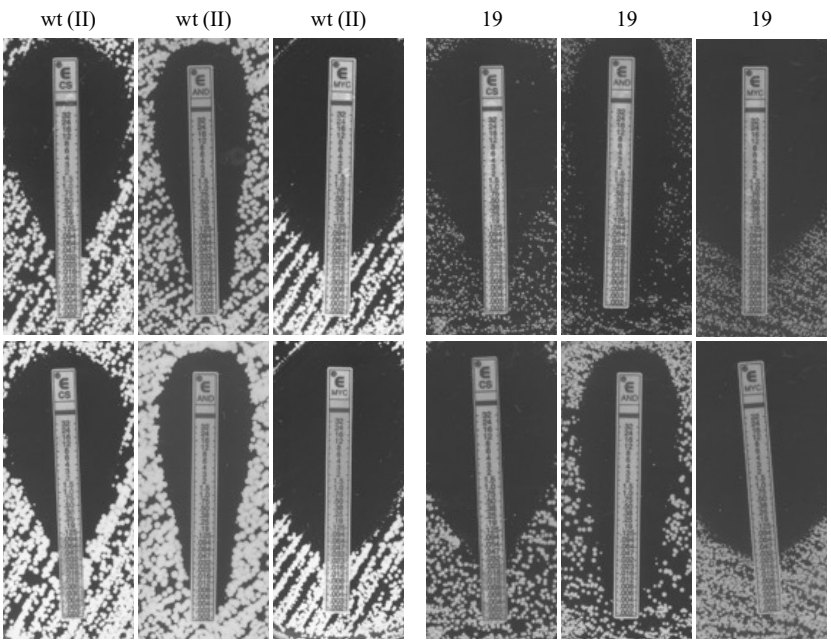

Strain (drug)	MIC
wt (CAS)	0.047
wt (ANF)	0.012
wt (MCF)	0.032
19 (CAS)	0.023
19 (ANF)	0.004
19 (MCF)	0.023

E)

clade	strain	MCF	CAS	ANF
I	1	0.380	0.090	0.190
I	2	1.520	0.510	1.470
I	3	0.750	0.330	1.000
I	4	1.000	0.330	0.730
I	5	0.510	0.250	0.730
I	6	0.510	0.250	0.500
III	7	0.120	0.060	0.050
III	8	0.660	0.500	0.060
III	9	0.660	0.500	0.760
III	10	0.660	1.000	0.380
III	11	0.660	0.500	0.030
III	12	1.320	0.760	0.380
IV	13	0.660	1.320	0.040
IV	14	1.000	1.320	0.020
IV	15	0.660	1.000	1.000
IV	16	0.660	1.320	0.120
IV	17	0.660	1.320	0.020
IV	18	1.320	2.000	0.170
II	19	0.719	0.489	0.333

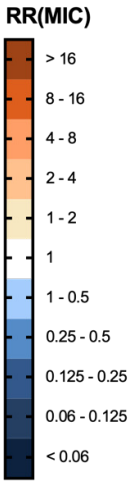

F)

clade	strain	MCF	CAS	ANF
I	1			
I	2			
I	3			
I	4			
I	5			
I	6			
III	7			
III	8			
III	9			
III	10			
III	11			
III	12			
IV	13			
IV	14			
IV	15			
IV	16			
IV	17			
IV	18			
II	19			

